

ARTICLE

Performance study of crack width calculation methods according to Eurocodes, *fib* model codes and the modified tension chord model

Otto Terjesen¹ | Gianclaudio Pinto² | Terje Kanstad³ | Reignard Tan^{3,4} 

¹University of Agder, Grimstad, Norway

²Implenia Norway AS, Oslo, Norway

³Norwegian University of Science and Technology, Trondheim, Norway

⁴Multiconsult AS, Oslo, Norway

Correspondence

Otto Terjesen, University of Agder, Jon Lilletuns vei 9, 4879 Grimstad, Norway.
Email: otto.terjesen@uia.no

Funding information

Norges Teknisk-Naturvitenskapelige Universitet; Universitetet i Agder

Abstract

This article investigates the accuracy of various crack width prediction models and the newly proposed modified tension chord model (MTCM). A large number of experimental crack widths have been collected from the literature, including 203 specimens of reinforced concrete (RC) members subjected to bending and tension. The prediction models are described with upcoming new formulations and database validation. The modeling uncertainty is found by comparing the predicted crack widths against experimental data obtained using a log-normal distribution. The results show that *fib* Model Code 2010 and MTCM provide the best crack width predictions of the collected databases; MTCM has the fewest mechanical simplifications of the investigated models and no empirical modifications for fitting towards experimental databases, in contrast to the approaches in Eurocode 2 and Model Code. However, the latter do predict the crack width to a reasonably good extent and are more suited for practical dimensioning than the MTCM. The findings in this article suggest that the MTCM should serve as a point of departure for further development of crack width calculation methods, and that it may have an extensive range of possible applications in the future.

KEYWORDS

bond stress distribution, concrete cover, crack stages, crack width, effective tension area, fitting of the databases by empirical modifications

1 | INTRODUCTION

Cracks are common in reinforced concrete (RC) structures, and usually occur with irregular distribution and different crack widths along an RC member. As long as the crack width remains within an acceptable range, these cracks neither impair the serviceability or bearing capacity, nor the durability of the structure (Leonhardt¹

and Beeby²). Strict crack width limits in RC structures often increase reinforcement amounts, and the economic consequences are significant.³ Extensive research has been carried out, and many approaches exist to predict the crack widths, but conversely, it is difficult to predict them consistently and accurately. This is reflected in the many techniques and methods proposed in the literature.⁴ There are, however, still substantial uncertainties

This is an open access article under the terms of the [Creative Commons Attribution](https://creativecommons.org/licenses/by/4.0/) License, which permits use, distribution and reproduction in any medium, provided the original work is properly cited.

© 2024 The Authors. *Structural Concrete* published by John Wiley & Sons Ltd on behalf of International Federation for Structural Concrete.

in the calculations, mainly due to the large-scale concrete structures, the large concrete covers applied in harsh environments, and the introduction of more eco-friendly modern concretes.⁵

The main objective of this article is to investigate the accuracy of the various calculation models and to shed light on ongoing discussions. This is performed by comparing the experimental crack widths reported with crack widths predicted by selected analytical calculation methods from design codes such as the present Eurocode 2 (EC2) and the draft for its new final version FprEC2 (2022),^{6,7} fib Model Code 2010 (MC2010) and its new draft 2020 (MC2020),^{8,9} the German National Annex to Eurocode 2 (DIN)¹⁰ and the recently published MTCM by Tan et al.¹¹ The different strategies used by the codes are categorized by Schlicke et al.¹² as either mechanical or calibrated models. The researchers behind MC2020 and FprEC2 have made their choices to improve the models. Still, large uncertainties remain, and the CEN member states must make their national application documents to FprEC2 in the coming years, and thus, more research is needed. Therefore, a database of 203 RC specimens of reinforced concrete (RC) members subjected to bending and tension has been collected from the literature with a total of 733 data points. All of the reported data was collected from various articles and books, with validation and control checks of the data for unreasonable values. The database validation was done by two different adjustments: one due to steel stress limitation and one due to a theoretical maximum mean crack width.

The present article is part of ongoing research activity related to the “Coastal Highway Route E39”, a project launched by the Norwegian Public Roads Administration (NPRA) and to MEERC (More Efficient and Environmental Road Construction) being carried out at the University of Agder. Furthermore, the project aims to provide guidelines and contribute to a more consistent and correct crack width prediction methodology for RC structures in Serviceability Limit States (SLS).

The main finding in this article is that MTCM, without any empirical calibration, performs as well as, or even better than, the investigated code type formulations, which all are calibrated towards similar databases as developed in this research study.

2 | ANALYTICAL CRACK WIDTH PREDICTION METHODS

In this article, the following design codes are applied to each experimental data series: Eurocode 2 (EC2),⁶ the new version of Eurocode 2 (FprEC2),⁷ fib Model Code 2010 (MC2010),⁸ the draft for the new fib Model

Code 2020 (MC2020),⁹ and the German National Annex (DIN).¹⁰ In addition, the modified tension chord model (MTCM) developed by Tan¹³ is included.

All of the investigated models derive crack width formulations that, in principle, are based on the same formulae:

$$w = S(\varepsilon_{sm} - \varepsilon_{cm}) \quad (1)$$

where w is the crack width, S is the crack spacing, and $(\varepsilon_{sm} - \varepsilon_{cm})$ is the difference between the mean steel and concrete strain over the transfer lengths between cracks, that is, over the crack spacing. The models apply different simplifications to determine the parameters, and the following section provides an overview of the formulations used by each model to determine the crack spacing, while the subsequent sections present the methods used to determine the strain difference.

Classical derivations of crack width formulas mainly stem from three theories: The no-slip theory is based on the assumption of a perfect bond between reinforcement and concrete. This assumption is based on the existence of internal cracks near the steel-concrete interface, occurring due to the strain incompatibility between reinforcement and concrete. It has been shown by Terjesen et al.¹⁴ and Cervenka et al.¹⁵ that good agreement between non-linear finite element analysis (NLFEA) and experimental crack widths of concrete beams can be achieved assuming a perfect bond between reinforcement and concrete. However, this is found by computational modeling with a concrete damage plasticity model where the fracture energy is the governing parameter for concrete cracking. The second theory is the bond-slip theory, in which a slip is assumed to occur between reinforcement and concrete. The slip is assumed to be at its maximum at the crack, and after a certain distance, it becomes zero, MTCM and similar models, that is, the tension chord model (TCM). However, as shown in this article, the MTCM also agrees with experimental results. The last theory combines the two theories and is applied by Eurocode 2 and fib Model Code.

In addition to the investigated models, there are other prediction models available in the literature, that is, Chavin et al.¹⁶ proposed a crack width model representing the stabilized cracking stage which is based on Beeby et al.^{17,18} who observed that the steel strain variation is linear on both sides of a crack. From tensile force equilibrium, it follows that the linear concrete strain variation is related to a constant bond-stress relation. The model by Chavin et al. applies empirical modifications to describe the increase in crack width caused by the concrete cover. The study is related to highly debated statements from Beeby^{17,19} that (a) cover is a more decisive parameter for

the prediction of crack width than the ratio ϕ/ρ_{eff} and that (b) bond-slip conditions of reinforcement exert a nil or negligible influence on crack widths.

The crack spacing prediction is a specific reference to reality derived from experiments, whereby statistical modification may address the prediction accuracy. The various models predict either a characteristic-, mean- or maximum crack width. These design models are based on the stabilized crack stage, that is, no significant increase in the formation of new cracks or decrease in crack spacing with increased loading should occur. In design, however, an argument made by the authors in¹² is that only the maximum crack width is essential and that we should evaluate this against the experiments, thus relating the crack width to the calculated transfer length instead of a designated crack spacing formula derived empirically from experiments. This statement stems from the fact that the calculated transfer lengths to each side of a crack are more critical than the crack spacing measured itself. This calls for a calculation model that can predict cracking in both the crack formation stage and the stabilized cracking stage, thus making S in Equation (1) a *transient* parameter explicitly dependent on the load level as well as the geometrical and material parameters.^{20,21} At best, determining a representative maximum crack spacing from the experiments is challenging due to the input data's range of expected sizes, such as tensile strength along the concrete member and bond properties along the rebars. It is also challenging to determine which current crack stage the RC member is in with load levels based on experimentally measured results, and reported crack spacings for members in bending are often mean values with both a mean and maximum crack width.

The MTCM proposed by (Tan)¹³ is an analytical calculation model based on solving the second-order differential equation (SODE) of the slip between rebar and concrete, to which the local bond-slip law according to MC2010 with adjusted parameters to account for the mechanical behavior of RC ties is applied. It yields closed-form solutions for the so-called comparatively lightly loaded member (CLLM) behavior being analogous to the crack formation stage and non-closed form solutions for the so-called comparatively heavily loaded member (CHLM) behavior being analogous to the stabilized cracking stage. It was derived based on the mechanical behavior of RC ties and has not been calibrated towards any experimental database, aiming to not limit the range of applicability regardless of geometrical and material parameters, in contrast to EC2 and MC2010. It was demonstrated in Reference 13 that the MTCM provides excellent potential for yielding consistent crack width predictions for large-scale concrete structures, that is,

large covers, large cross-section dimensions and large reinforcement amounts. However, the non-closed form solutions for the CHLM behavior cannot directly figure as a code-type replacement for EC2 or MC2010 yet. Regardless, it can be applied at the project level, or it can be included in the national application documents of a country.

2.1 | Crack spacing

The applied methods predict the maximum crack spacing assuming that the concrete stress between two cracks can never be greater than its tensile strength. As the only exceptions, FprEC2 and MC2020 predicts the mean value and applies statistical modifications to predict the maximum crack width.

In the location of the crack, with corresponding steel stress, two different crack stages may occur, namely, (a) a single crack stage occurring when the steel force in the crack can be re-transferred entirely back into the cross-section without a new crack formation and (b) stabilized crack stage occurring when crack formation has progressed to such an extent that the steel strain between two adjacent cracks is greater than the ultimate tensile strain of concrete ($\epsilon_c = f_{ct}/E_c$). Each solution strategy is in agreement with the theoretical grounds (Equation 1) for calculating the crack width; however, models differ in estimating crack spacing and the strain difference between the concrete and reinforcement.

2.2 | Differences in steel and concrete strains

For determining the difference in mean steel and concrete strain at a stabilized crack pattern, the design codes^{6–10} use the expression in Equation (2).

$$\epsilon_{sm} - \epsilon_{cm} = \frac{\sigma_s - k_t \frac{f_{ctm}}{\rho_{\text{eff}}} (1 + \alpha * \rho_{\text{eff}})}{E_s} \quad (2)$$

where σ_s is the stress in the tensile reinforcement assuming a cracked section; k_t is a factor describing the effect of the duration of the load (0.6 for short-term loading and 0.4 for long-term loading); f_{ctm} is the mean tensile strength of concrete; ρ_{eff} is the effective reinforcement ratio, defined as $A_s/A_{c,\text{eff}}$; $A_{c,\text{eff}}$ is the effective tension area with an effective height $h_{c,\text{eff}}$; α is the modular ratio of steel and concrete defined as $\frac{E_s}{E_{cm}}$.

The k_t factor used in this article comparing theoretical and experimental results is the short-term value;

however, DIN use 0.4 for both short- and long-term load cases.

For the crack formation stage, EC2 and DIN use Equation (3) below, while MC2010 and MC2020 uses Equation (4) and FprEC2 with β equal to k_t defined above. Equations (3) and (4) defines the lower boundary for the difference in mean strains.

$$\varepsilon_{sm} - \varepsilon_{cm} \geq \frac{0.6 * \sigma_s}{E_s} \quad (3)$$

$$\varepsilon_{sm} - \varepsilon_{cm} \geq \frac{(1 - \beta) * \sigma_s}{E_s} \quad (4)$$

2.3 | Tension chord models

The TCM^{22,23} was developed in the 1990s at ETH Zurich. It models structural elements loaded in tension, including the effect of the bond between reinforcement and concrete, that is, the tension stiffening effect with only the magnitudes of the bond stresses as empirical parameters. The bond-slip behavior $\tau_b - u$ is assumed to be rigid-perfectly plastic, with a value $\tau(u) = \tau_{b0} = 2f_{ct}$ for regions where the reinforcement stresses are below yielding and $\tau(u) = \tau_{b1} = f_{ct}$ after the onset of yielding. These regions are visualized in Figure 1.

The model assumes that the nominal bond stresses (τ_b) are independent of the slip (u) and instead step-wise dependent on steel stress (σ_s), that is, $\tau_b(\sigma_s)$. This assumption enables the kinematic relations of a differential element of a reinforcing bar embedded in concrete to be expressed as:

$$\frac{du(x)}{dx} = \varepsilon_s(x) - \varepsilon_c(x) \quad (5)$$

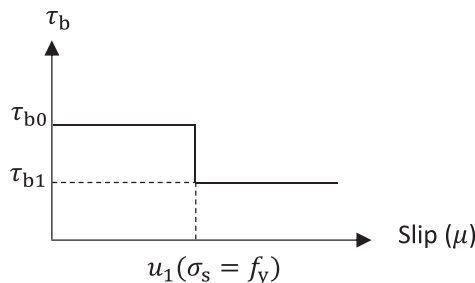


FIGURE 1 Definition of the constitutive model used in TCM before and after yielding.

Equilibrium conditions of the same element can be expressed as:

$$\frac{d\sigma_s(x)}{dx} = \frac{4\tau_b(u(x))}{\phi_s} = \frac{4\tau_b}{\phi_s} \quad (6)$$

with $\varepsilon_s(x)$, $\varepsilon_c(x)$ = steel and concrete strains along the reinforcement bar, $\sigma_s(x)$, $\tau_b(x)$ = steel stress and bond stress along the reinforcement bar, u = slip between reinforcing bar and concrete, ϕ_s = reinforcement bar diameter. With the assumption that bond stress is entirely determined by steel stress at a specific location (known by equilibrium), the steel stress can be determined by:

$$\sigma_s(x) = \sigma_{sr} - \frac{4\tau_b x}{\phi_s} \quad (7)$$

with $\sigma_{sr} = F/A_s$ = steel stress at the crack. The steel stress in Equation (7) yields a linear decrease in the steel stress from the crack to the middle of the cracked element caused by bond stresses.

The general expression for crack spacing for a stabilized crack stage is found by equilibrium considerations of a reinforced concrete tie between two cracks and is visualized in Figure 2 and deduced in the following:

$$\sigma_{sr} A_s = \sigma_s (S_r/2) A_s + f_{ctm} (A_c - A_s) \quad (8)$$

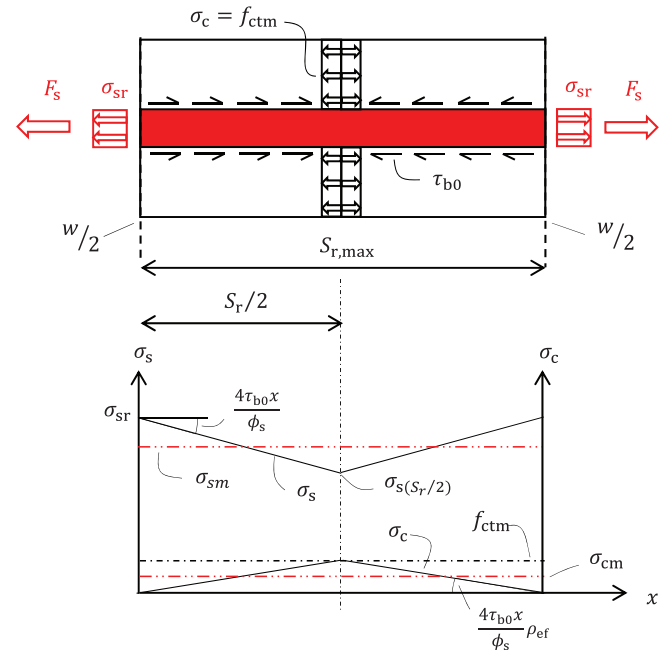


FIGURE 2 Distribution of steel and concrete stresses over the cracked RC-tie according to TCM below steel yielding for a stabilized crack pattern.

$$f_{ctm}(A_c - A_s) = \sigma_{sr}A_s - \sigma_s(S_r/2)A_s = \tau_{b0}n\pi\phi_s \frac{S_r}{2} \quad (9)$$

Introducing an effective concrete area $\rho_{ef} = A_s/A_c$ the concrete area can be expressed as:

$$A_c = \frac{A_s}{\rho_{ef}} \quad (10)$$

where $\rho_{ef} = n\phi^2\pi/4A_c$. By inserting Equation (10) into Equation (9), solving for crack spacing $S_{r,max}$ yields the maximum crack spacing as:

$$S_{r,max} = S_{TCM} = \frac{f_{ctm}\phi_s(1-\rho_{ef})}{2\tau_{b0}\rho_{ef}} \quad (11)$$

For a stabilized crack pattern, the maximum crack width can be expressed by the crack spacing and the difference in steel and concrete deformation. For the TCM, this yields:

$$w = \delta_s - \delta_c = S_{TCM}(\varepsilon_{sm} - \varepsilon_{cm}) \quad (12)$$

By integrating the steel strains over the crack spacing S_{TCM} yields the mean steel strain as:

$$\varepsilon_{sm} = \frac{1}{S_{TCM}} \int_0^{S_{TCM}} \varepsilon_s(x) dx = \frac{1}{E_s} \left(\sigma_{sr} - \frac{\tau_{b0} S_{TCM}}{\phi_s} \right) \quad (13)$$

and mean concrete strains.

$$\varepsilon_{cm} = \frac{1}{S_{TCM}} \int_0^{S_{TCM}} \varepsilon_c(x) dx = \frac{1}{E_c} \rho_{ef} \frac{\tau_{b0} S_{TCM}}{\phi_s} \quad (14)$$

Furthermore, by inserting Equations (13) and (14) into Equation (12), we can now express the maximum crack width by TCM as:

$$w = S_{TCM} \left[\frac{1}{E_s} \left(\sigma_{sr} - \frac{\tau_{b0} S_{TCM}}{\phi_s} \right) - \frac{1}{E_c} \rho_{ef} \frac{\tau_{b0} S_{TCM}}{\phi_s} \right] \quad (15)$$

The German code DIN applies the same equilibrium shown in Equations (5)–(9) but does not include the steel area in Equation (9), yielding the following expression for the maximum crack spacing.

$$S_{DIN} = \frac{f_{ctm}\phi_s}{2\tau_{b0}\rho_{ef}} \quad (16)$$

DIN then assume $\tau_{b0} = 1.8f_{ctm}$ and inserting this into Equation (13) yields the maximum crack spacing shown in Table 1.

$$S_{max} = \frac{\phi_s}{3.6\rho_{ef}} \quad (17)$$

TABLE 1 Summary of crack spacing formulae in the design codes and MTCM.

Code	Crack spacing formula	Information
EC2	$S_{r,max} = k_3c + k_1k_2k_4 \frac{\phi}{\rho_{eff}}$	$k_1 = 0.8, k_3 = 3.4, k_4 = 0.425$ $k_2 = 0.5/1$ (bending/tension)
prEC2	$S_{r,max,cal} = 1.5c + \frac{k_{fl}k_b}{7.2} \frac{\phi}{\rho_{eff}} \leq \frac{1.3}{k_w}(h-x)$	$k_b = 0.9$ $k_{fl} = \frac{1}{2} \left(1 + \frac{h-x_g - h_{c,eff}}{h-x_g} \right); k_w = 1.7$
MC2010	$S_{r,max} = 2l_{s,max} = 2 \left[kc + \frac{1}{4} \frac{f_{ctm}}{\tau_b} \frac{\phi}{\rho_{eff}} \right]$	$k = 1$ $\tau_b = 1.8f_{ctm}$
MC2020	$S_{r,max} = \beta_w \left(k_c c + k_{\theta/\rho} k_{fl} k_b \frac{f_{ctm}\phi}{\tau_b \rho_{s,eff}} \right)$	$k_c = 1.5, k_{\theta/\rho} = 0.25,$ $k_b = 0.9, \tau_b = 1.8f_{ctm}$ $k_{fl} = \frac{1}{2} \left(1 + \frac{h-x_g - h_{c,eff}}{h-x_g} \right)$ $\beta_w = 1.7$ for stabilized cracking stage and 2.0 for the crack formation stage
DIN	$S_{r,max} = \frac{\phi}{3.6\rho_{eff}} \leq \frac{\sigma_s \phi}{3.6f_{ctm}}$	
MTCM ^a	$S_{r,CHLM} = \frac{1}{\delta} \left[\frac{f_{ctm}}{E_{cm}} \frac{1+\xi}{\xi\psi} \left(\frac{1}{2\gamma} \right)^{\frac{2\delta}{\beta}} \right]^{\frac{2\delta}{\beta}}$	CHLM (Maximum crack spacing in a stabilized cracking stage)
	$S_{r,CLLM} = 2 \cdot \frac{1}{\delta} \left[\varepsilon_{sr} \left(\frac{1}{2\gamma} \right)^{\frac{1}{2\delta}} \right]^{\frac{2\delta}{\beta}}$	CLLM (Crack formation stage where the maximum crack spacing is equal to two times the transfer length)

^aParameters are explained in Chapter 3.3.

2.3.1 | Modified tension chord model

The MTCM was developed by Tan in 2019.¹³ It is based on solving the Second Order Differential Equation (SODE) for the slip in Equation (18) analytically.

$$\frac{d^2 u}{dx^2} - \chi \tau(u) = 0 \quad (18)$$

where $\chi = (\sum \pi \phi_s / A_s E_s)(1 + \xi)$ is a constant for equivalent cross-sections when using the SODE for the slip with the parameters ϕ_s , A_s , and E_s being the diameter, area and the Young's modulus for the rebar. Furthermore, the other constants are defined as $\xi = \alpha_E \rho_s / \psi$, $\alpha_E = E_s / E_c$, and $\rho_s = A_s / A_c$, with A_c being the sectional area of the RC tie and E_c the Young's modulus for concrete. The parameter $\psi \leq 1.0$ is a factor accounting for the fact that plane sections do not remain plane in RC ties.^{24,25} It was observed by Tan et al.¹¹ that $\psi = 0.7$ seemed reasonably independent of geometry and load level.

The model considers the same equilibrium, compatibility and linear elastic material laws for steel and concrete as the TCM for a differential element in an RC tie. However, it assumes that the nominal bond stresses (τ_b) are directly dependent on the slip (u) as visualized in Figure 3, and not rigid-perfectly plastic as for the TCM. Solving for the slip in Equation (18) analytically requires using a local bond-slip law. The MTCM applies the local bond-slip law first proposed by Eligehausen et al.²⁶ and later adopted by MC2010 in Equation (19).

$$\tau(u) = \tau_{\max} \left(\frac{u}{u_1} \right)^\alpha \quad (19)$$

where u is the slip at the load level and the empirical factors $\tau_{\max} = 5$ MPa, $u_1 = 0.1$ mm, and $\alpha = 0.35$ are assumed to be representative of the behavior of RC ties. These factors were determined in Reference 27, with $\tau(u)$ representing a sort of the mean of local bond-slip curves for an arbitrary RC tie.

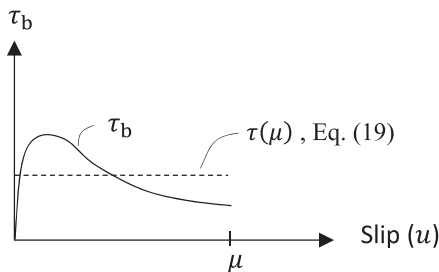


FIGURE 3 Definition of the constitutive model used in MTCM.

Inserting Equation (19) into (18) yields the SODE.

$$\frac{d^2 u}{dx^2} - \chi \frac{\tau_{\max}}{u_1^\alpha} u^\alpha = 0 \quad (20)$$

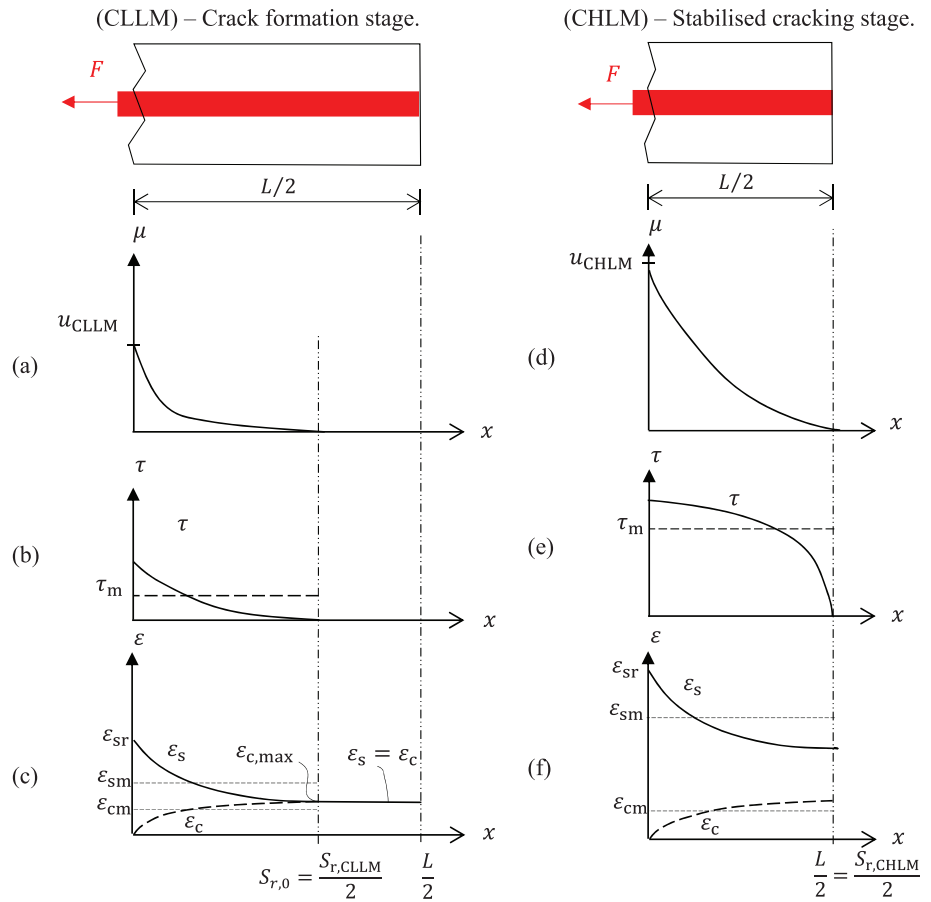
The nonlinear homogenous SODE in Equation (20) can now be solved analytically as described in Reference 11. Because the main application of the model is within SLS, the following sections focus on steel strains and stresses below yielding. In this state, the MTCM gives two sets of boundary conditions grouped by the two concepts of comparatively lightly loaded members (CLLM) and comparatively heavily loaded members (CHLM). These concepts are analogous to the crack formation stage (CLLM) and stabilized cracking stage (CHLM). The concept of CLLM is depicted in Figure 4a–c, in which the transfer length $S_{r0} = S_{r,CLLM}/2$ denotes the abscissa, where steel and concrete strains become compatible and consequently zero slip. This point moves towards the symmetry section $L/2$ with increasing load and a new crack is formed at the location where the concrete stresses exceed the tensile strength of the concrete, that is, $S_{r,CLLM}/2 = L/2$ if $\epsilon_c(S_{r,CLLM}/2) = \epsilon_{c,max} \geq \epsilon_{ctm} = f_{ctm}/E_c$. Afterwards, the concept of CHLM depicted in Figure 4d–f governs with $S_{r,CHLM}$ as the crack spacing. This concept now yields the response for the cracked member, in which it is observed that the distribution of steel and concrete strains remains incompatible over the entire crack spacing, and the slip is zero only at the symmetry section, as depicted in Figure 4d.

The solution of the SODE in Equation (20) can now be obtained by solving the equation for two sets of boundary conditions for the case of CLLM and CHLM. For CLLM, the slip and difference in strains are zero at the end of the transfer length s_{r0} . For CHLM, the slip is zero at the symmetry section $L/2$, however, the difference in strains is always larger than zero. With the chosen bond-slip law in Equation (19), the maximum slip at the loaded end in the case of CLLM Figure 4a can be found directly from the closed-form solution expressed as:

$$u_{r,CLLM} = \left(\frac{\epsilon_{sr}^2}{2\gamma} \right)^{\frac{1}{\beta}} \quad (21)$$

with the constant $\gamma = \chi \tau_{\max} / (\beta u_1^\alpha)$, $\chi = (\sum \pi \phi_s / A_s E_s)(1 + \xi)$, $\beta = 1 + \alpha$ and the bond-slip parameters $u_1 = 0.1$ and $\alpha = 0.35$. For the case of CHLM, the maximum slip $u_{r,CHLM}$ depicted in Figure 4d has to be determined iteratively as a function of steel strain at the crack ($\epsilon_{sr} = F/A_s$) due to the non-closed form solution of the SODE for this set of boundary conditions. The solution procedure for

FIGURE 4 Distribution of slip, bond stress, steel and concrete strains over the cracked RC-tie for the concepts (a–c) CLLM and (b–f) CHLM.



determining the maximum slip is provided in Reference 11. Note that the slip in Equation (20) for both concepts directly depends on the reinforcement ratio and rebar size through the constant χ .

For CLLM, the crack spacing ($S_{r,CLLM}$) expressed in Equation (22) is twice the theoretical transfer length of each side of a crack where steel and concrete strains become compatible in Figure 4c. The transfer length directly depends on the steel stain at the crack, which makes the transfer length transient.

$$S_{r,CLLM} = 2 \cdot \left[\frac{1}{\delta} \left[\epsilon_{sr} \left(\frac{1}{2\gamma} \right)^{\frac{1}{2\beta}} \right]^{\frac{2\beta}{\beta-1}} \right] \quad (22)$$

In the case of CHLM, the steel and concrete strains in Figure 4f are found by integrating over the transfer length, which is defined as half the crack spacing and the maximum crack spacing ($S_{r,CHLM}$) is given by:

$$S_{r,CHLM} = \frac{1}{\delta} \left[\frac{f_{ctm}}{E_{cm}} \frac{1+\xi}{\xi\psi} \left(\frac{1}{2\gamma} \right)^{\frac{1}{2\beta}} \right]^{\frac{2\beta}{\beta-1}} \quad (23)$$

where $\delta = (1 - \alpha)/2$.

The mean steel and concrete strains for the CLLM behavior can be expressed as:

$$\epsilon_{sm} = \frac{1}{S_{r,CLLM}} \frac{\xi \epsilon_{sr} S_{r,CLLM} + 2u_{r,CLLM}}{1 + \xi} \quad (24)$$

$$\epsilon_{cm} = \frac{\psi \xi}{S_{r,CLLM}} \frac{\epsilon_{sr} S_{r,CLLM} - 2u_{r,CHLM}}{1 + \xi} \quad (25)$$

and for CHLM:

$$\epsilon_{sm} = \frac{1}{S_{r,CHLM}} \frac{\xi \epsilon_{sr} S_{r,CHLM} + 2u_{r,CLLM}}{1 + \xi} \quad (26)$$

$$\epsilon_{cm} = \frac{\psi \xi}{S_{r,CHLM}} \frac{\epsilon_{sr} S_{r,CHLM} - 2u_{r,CHLM}}{1 + \xi} \quad (27)$$

with the crack width for both cases expressed as:

$$w_{CLLM} = S_{r,CLLM} (\epsilon_{sm} - \epsilon_{cm}) \quad (28)$$

$$w_{CHLM} = S_{r,CHLM} (\epsilon_{sm} - \epsilon_{cm}) \quad (29)$$

In summary, both of the concepts of CLLM (crack formation stage) and CHLM (stabilized cracking stage) account for rebar size and reinforcement ratio for calculating the slip, which is nonlinear, as seen in Figure 4a, d. However, the main difference between the two is that the steel and concrete strains become incompatible over the entire bar length in the case of CHLM, as depicted in Figure 4f.

2.3.2 | The conceptual difference between the TCM and MTCM

The TCM assumes a simple step-wise, rigid-perfectly plastic bond-slip law that yields a slip (u) independent of the load level in regions below and above yielding in the reinforcement, as seen in Figure 1. The steel stress between two cracks is found by considering equilibrium, as shown in Equations (5)–(14), and the crack width is found as the difference between the steel and concrete deformation in Equation (15).

For the MTCM, the bond stress varies over the element length depending on the load level according to a given bond-slip relation. The maximum slip u_r , which is obtained in Equation (21) in the case of CLLM and iteratively in the case of CHLM, is required to calculate steel and concrete strains in Equations (24)–(27). The crack width is found by multiplying the strain difference with twice the transfer length for the case of CLLM or the crack spacing in CHLM, as shown in Equations (28) and (29).

The conceptual difference between TCM and MTCM is visualized in Figure 5 for steel stresses prior to yielding and a stabilized crack pattern (CHLM), in which the continuous and dashed lines represent steel strains ϵ_s and the corresponding concrete strains ϵ_c . Linear curves show that the strains vary over the bar length with a constant slope of $4\tau_{b0}/\phi_s$ for the TCM, while nonlinear strain distributions, in general, are observed for the MTCM.

2.4 | New parameters in FprEC2 and MC2020

FprEC2 and MC2020 include several modifications of both the crack width and maximum crack spacing formulas based on the work conducted by Caldentey et al.²⁸

In MC2020, the factor k_{fl} is intended to account for the effect of stress distribution within the effective concrete tensile area.

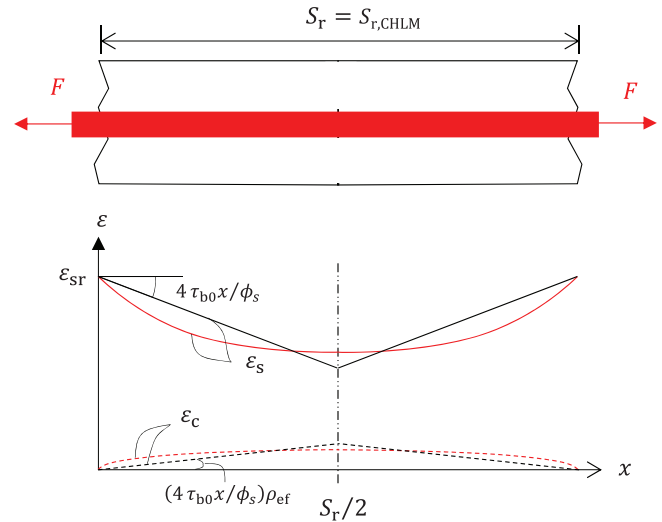


FIGURE 5 Concept of steel and concrete strain distribution over the bar length for a stabilized crack pattern below reinforcement yielding of CHLM. Linear strain distribution represents the concept of TCM, while Nonlinear distribution represents the concept of MTCM.

$$k_{fl} = \frac{1}{2} \left(1 + \frac{h - x_g - h_{c,ef}}{h - x_g} \right) \quad (30)$$

Equation (30) is valid for $h > x_g$, where x_g is the height of the compression zone of the uncracked section, and $h_{c,ef}$ is the height of the effective tensile area. The value of the expression of k_{fl} approaches 1 for pure tension (neutral axis depth $x_g = 0$) and 0.5 for bending when $h_{c,eff}$ is equal to the entire tensile zone ($h - x_g$).

Furthermore, for a rectangular cross-section under pure flexure ($x_g = h/2$) Equation (30) can be simplified to.

$$k_{fl} = \frac{h - h_{c,ef}}{h} \quad (31)$$

The factor k_b accounts for the effects of the casting process on the crack spacing, depending on whether the tensile zone is cast in a poor or good position in regard to the bond strength.

$$k_b = \begin{cases} 1.2 & \text{for poor bond conditions} \\ 0.9 & \text{for good bond conditions} \end{cases} \quad (32)$$

In the crack width formula, a new parameter introduced in FprEC2 is the curvature factor $k_{1/r}$ describing that, in bending, the value of the crack width increases proportionally with the distance from the tensile reinforcement.

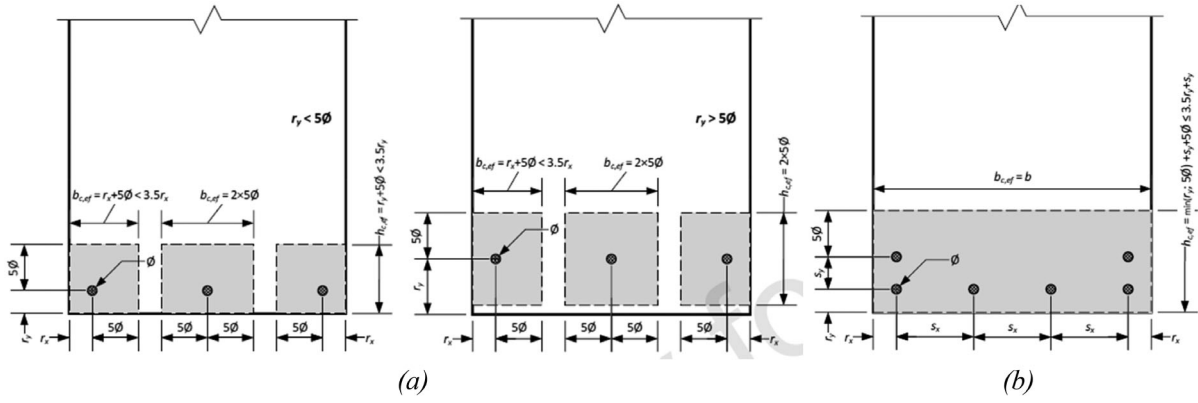


FIGURE 6 MC2020: Effective tension area of concrete (a) isolated bars and (b) group of bars.⁹

FIGURE 7 FprEC2: Effective tension area of concrete in bending (a) group of bars, (b) isolated bars and (c) circular cross-section.²⁹

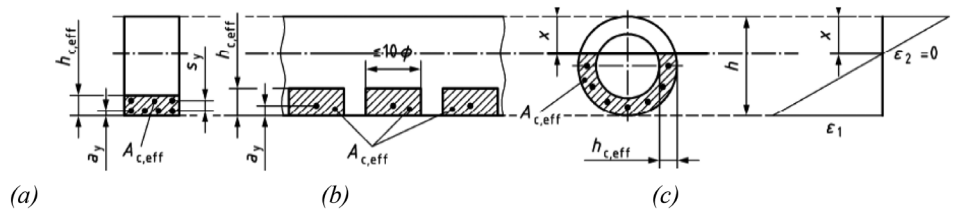
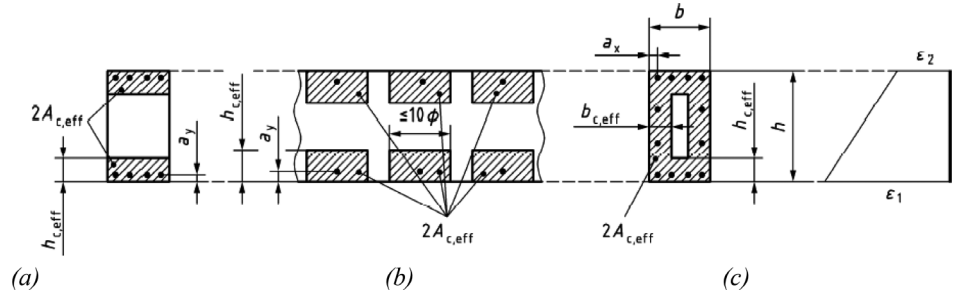


FIGURE 8 FprEC2: Effective tension area of concrete of both faces in tension (a, b) group of bars and (c) isolated bars.²⁹



$$k_{1/r} = \frac{h - x_g}{d - a_{y,i} - x_g} \quad (33)$$

where d is the effective height, h is the height of the section, while $a_{y,i}$ is the cover plus half the rebar size.

Additional changes for the effective tension area ($A_{c,ef}$), represented by the effective height ($h_{c,ef}$) for single or layered reinforcement bars, are described by Equations (34a) and (34b) for MC2020, visualized in Figure 6 and Equations (34c) and (34d) for FprEC2, visualized in Figures 7 and 8.

$$h_{c,ef} = \min(r_y + 5\phi; 10\phi; 3.5r_y) \leq h - x \quad (34a)$$

$$h_{c,ef} = \min(r_y + 5\phi; 10\phi; 3.5r_y) + (n_l - 1)s_y \leq h - x \quad (34b)$$

$$h_{c,ef} = \min\left(a_y + 5\phi; 10\phi; 3.5a_y; h - x; \frac{h}{2}\right) \quad (34c)$$

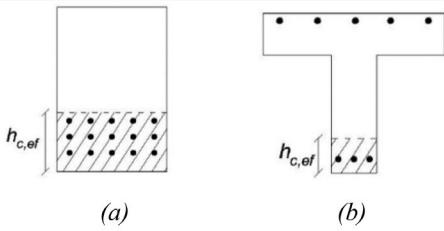
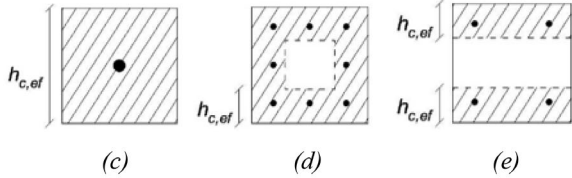
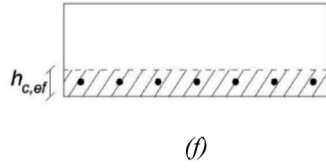
$$h_{c,ef} = \min\left\{\min\{a_y + 5\phi; 10\phi; 3.5a_y\} + (n_l - 1)s_y; h - x; \frac{h}{2}\right\} \quad (34d)$$

In which, r_y and a_y are the distance from the concrete surface to the centre of the bar in the y -direction and n_l is the number of reinforcement layers.

3 | DATABASE

An extensive database was created by collecting a large number of experimental results from the literature on reinforced concrete (RC) members subjected to bending and tension. The data was sorted into three categories before investigating the modeling uncertainties. In most references, the specimens were investigated throughout

TABLE 2 Overview of the databases with corresponding cross-sections.

First database: 97 experiments with beams in bending (429 data points)	
<ul style="list-style-type: none"> Hognestad,³⁰ (35 beams) CUR report,³¹ (24 beams) Rüsch – Rehm,³² (14 beams) Clark,³³ (24 beams) 	
Second database: 73 experimental RC ties (104 data points) of RC ties in pure tension	
<ul style="list-style-type: none"> Hartl,³⁴ (49 ties) Garcia et al.³⁵ (4 ties) Rimkus et al.³⁶ (10 RC ties) Wu & Gilbert,³⁷ (2 RC ties) Tan et al.³⁸ (8 RC ties) 	
Third database: 33 experimental slabs in bending (200 data points)	
<ul style="list-style-type: none"> CUR report,³¹ (7 slabs) Clark,³³ (26 slabs) 	

the serviceability limit state and, occasionally, until yielding or failure occurred. Stress levels and measurement results were reported, such as steel and concrete strains, mean and maximum crack widths, and average crack spacing. For several experimental investigations, results at different load steps were available from the literature.

The three databases are presented in Table 2:

1. Beams in bending
2. RC tensile ties
3. Slabs in bending

The effective heights $h_{c,ef}$ of the cross-sections were calculated following the procedures in the calculation models. For the MTCM applied to the first and third databases related to bending, the effective height was calculated according to EC2.

Figure 9 shows an overview of the databases' cross-section heights, with the first database primarily consisting of heights in the range of 500–600 mm, the second database in the range of 50–100 mm and the third database in the range of 150–200 mm. As shown in Figure 10a, the cover sizes for the first and second

databases are in the range of 10–50 mm, while in the third database, the slabs have a cover in the range of 10–30 mm. Figure 10b shows that the reinforcement ratio varies significantly between 1% and 6% for all three databases.

3.1 | Adjustment of the databases

Almost no maximum crack spacings for beams and slabs in bending are reported in the database. In contrast, the average crack spacing is registered based on each author's subjective interpretation and choices. Hognestad³⁰ reported average crack spacing based on primary cracks and disregarded secondary cracks, that is, those close to the major cracks were excluded from the calculations. Rusch & Rehm³² did not calculate crack spacing but made a detailed report of crack widths measured at five different points along the concrete face and their location along the beam length. From that, average crack spacing was calculated by disregarding secondary cracks. Clark³³ reported average crack widths calculated from all cracks (major and secondary) in the constant moment zone. In

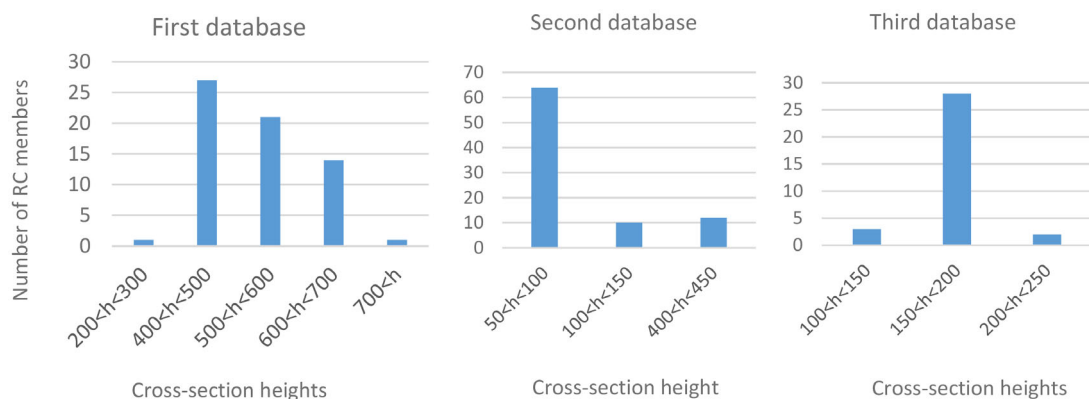


FIGURE 9 Distribution of cross-section heights in the databases.

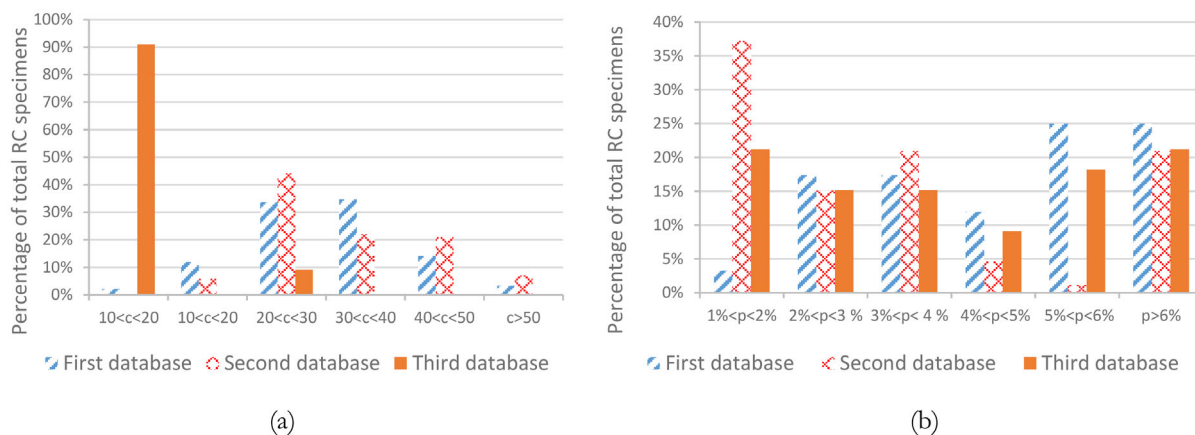


FIGURE 10 Distribution of (a) concrete cover and (b) of the reinforcement ratio, using the effective height set by EC2 for RC members in the databases.

In addition, the crack widths and spacing in the location for bending and shear cracks were included if the crack spacing was less or equal to 6 inches (152.4 mm) in this zone. Therefore, verifying which cracks (major and secondary) are included or excluded is difficult due to limited information or lack thereof. There are also uncertainties regarding how the measured crack widths and spacings were found across the RC member's width and length. In some cases, it is also uncertain if the reported crack width is a single point or an average of more readings, that is, across the member's width at the bottom outermost concrete face. Hence, database adjustments are performed to obtain consistent comparisons of predictions from calculation models with experimental results.

3.1.1 | First adjustment

In SLS, it is uncommon to have reinforcement stress above 300 MPa; therefore, the first adjustment was

excluding data with stresses larger than this. This requirement results into a reduction of data on 27%, 41%, and 55% for the three respective databases.

3.1.2 | Second adjustment

A second adjustment was performed to further benchmark the experimental results by considering mean crack width and spacings, and investigating if they were unreasonably large. The focus on mean values is due to the literature's lack of reported maximum crack spacings. Using the theoretical framework of all the investigated methods described by Equation (1), we should be able to predict an upper limit of the mean crack width by neglecting bond stresses between steel and concrete or, more rigorously, the tension stiffening effect, as given in Equation (35).

$$w_{\text{mean,max}} = \varepsilon_{\text{sr}} S_{\text{exp,mean}} \quad (35)$$

TABLE 3 Modeling uncertainty.

Model	θ_{mean}	θ_{var}	θ_{SD}	θ_{COV}	θ_{min}	θ_{max}	$n(\theta > 1)$	$(\theta > 1) \%$
<i>(a) Beams subjected to bending, 429 data points</i>								
MTCM	1.05	0.083	0.309	0.294	0.433	3836	225	52.4
EC2	1.31	0.073	0.360	0.275	0.598	4857	361	84.1
FprEC2	1.34	0.060	0.335	0.250	0.651	4043	368	85.8
MC2010	1.11	0.065	0.286	0.258	0.439	3653	253	59.0
MC2020	1.33	0.059	0.327	0.246	0.651	4043	366	85.3
DIN	1.81	0.116	0.634	0.351	0.586	4852	417	97.2
<i>(b) 315 data points, $\sigma_{\text{sr}} \leq 300 \text{ Mpa}$</i>								
MTCM	1.02	0.074	0.284	0.278	0.375	2199	155	49.2
EC2	1.30	0.073	0.358	0.276	0.598	4794	262	83.2
FprEC2	1.36	0.063	0.345	0.255	0.651	3359	270	85.7
MC2010	1.11	0.066	0.288	0.261	0.439	2734	187	59.4
MC2020	1.34	0.061	0.336	0.251	0.651	3359	268	85.1
DIN	1.83	0.123	0.663	0.362	0.586	4649	304	96.5
<i>(c) 227 data points, results included if $w_{\text{mean,exp}} < S_{\text{mean}} \epsilon_{\text{sr}}$</i>								
MTCM	0.98	0.075	0.278	0.278	0.433	2187	98	43.3
EC2	1.27	0.080	0.369	0.290	0.598	4794	178	79.5
FprEC2	1.40	0.069	0.374	0.266	0.746	3605	194	86.6
MC2010	1.10	0.074	0.304	0.277	0.439	2734	128	57.1
MC2020	1.36	0.064	0.349	0.257	0.651	3359	191	85.3
DIN	1.69	0.116	0.592	0.350	0.586	4522	213	95.1

where ϵ_{sr} is the steel strain at the load level of the reported mean crack spacing $S_{\text{exp,mean}}$. Data points which had measured mean crack widths larger than $w_{\text{mean,max}}$ were excluded from the database. An aspect of this adjustment is due to uncertainties if shrinkage could have affected the experiments. Significant shrinkage might result in a negative tension stiffening, but by excluding tests with reported mean crack widths larger than Equation (35), the tension stiffening (TS) factor is always ≤ 1.0 , and the shrinkage problem is assumed to be accounted for.

4 | RESULTS

The accuracy of the investigated crack width prediction models was determined by applying the concept of modeling uncertainty according to the method provided by Engen et al.³⁸ and Tan et al.³⁷ The method assumes a log-normal distribution, according to the guidelines of the JCSS Probabilistic Model Code³⁹ and is thereby considering the natural logarithm of theta (θ) as a normal distribution and is determined as:

$$\theta = \frac{w_{\text{exp}}}{w_{\text{cal}}} \quad (36)$$

where w_{exp} is the experimental crack width reported from the experiments and w_{cal} the crack width calculated by the various methods. The uncertainty, determined by the quality of a model, represents the lack of knowledge and is called epistemic uncertainty. The best agreement between the prediction models and the experiment is obtained when θ is close to 1.0. Tables 3–5 show the statistical properties of the modeling uncertainty for each calculation model for the databases previously described and are graphically presented in Figures 12–16 with the mean value (θ_{mean}), the variance (θ_{var}), the standard deviation (θ_{SD}), the coefficient of variation (θ_{COV}), the minimum (θ_{min}) and maximum (θ_{max}) values of θ , and the number of observations n for which the crack widths measured exceed the maximum crack widths predicted ($\theta > 1$).

- Table 3(a) shows the statistical properties of the modeling uncertainty from the first database consisting of 92 RC beams and 429 data points.

TABLE 4 Modeling uncertainty.

Model	θ_{mean}	θ_{var}	θ_{SD}	θ_{COV}	θ_{min}	θ_{max}	$n(\theta > 1)$	$(\theta > 1) \%$
<i>(a) RC ties in tension 104 data points</i>								
MTCM	0.86	0.131	0.320	0.374	0.17	2.04	18	17.3
EC2	0.64	0.113	0.221	0.345	0.10	1.62	2	1.9
FprEC2	1.03	0.093	0.321	0.312	0.23	2.34	34	32.7
MC2010	0.96	0.110	0.327	0.340	0.20	2.58	27	26.0
MC2020	1.01	0.108	0.342	0.338	0.19	3.01	33	31.7
DIN	1.18	0.140	0.459	0.388	0.19	2.29	51	49.0
<i>(b) 61 data points, $\sigma_{\text{sr}} \leq 300 \text{ Mpa}$</i>								
MTCM	0.92	0.152	0.372	0.405	0.17	2.04	16	26.2
EC2	0.73	0.153	0.298	0.406	0.10	1.61	2	3.3
FprEC2	1.07	0.106	0.358	0.335	0.23	2.32	31	50.8
MC2010	1.01	0.124	0.368	0.363	0.20	2.57	25	41.0
MC2020	1.08	0.119	0.386	0.356	0.23	2.99	31	50.8
DIN	1.17	0.144	0.459	0.394	0.19	2.28	38	62.3

TABLE 5 Modeling uncertainty.

Model	θ_{mean}	θ_{var}	θ_{SD}	θ_{COV}	θ_{min}	θ_{max}	$n(\theta > 1)$	$(\theta > 1) \%$
<i>(a) Slabs subjected to bending, 200 data points</i>								
MTCM	0.90	0.113	0.313	0.346	0.21	2.14	63	31.5
EC2	1.80	0.189	0.823	0.456	0.32	5.43	178	89.0
prEC2	1.59	0.163	0.667	0.421	0.30	4.39	174	87.0
MC2010	1.20	0.165	0.508	0.423	0.29	3.31	128	64.0
MC2020	1.72	0.152	0.698	0.405	0.34	4.39	182	91.0
DIN	1.75	0.255	0.943	0.539	0.25	5.09	156	78.0
<i>(b) 90 data points, results included if $\sigma_{\text{sr}} \leq 300 \text{ MPa}$ and $w_{\text{mean, exp}} \leq S_{\text{mean}} \epsilon_{\text{sr}}$</i>								
MTCM	0.82	0.125	0.299	0.365	0.21	1.37	17	18.9
EC2	1.54	0.197	0.719	0.467	0.32	2.90	72	80.0
prEC2	1.35	0.176	0.592	0.439	0.30	2.55	68	75.6
MC2010	1.05	0.160	0.436	0.416	0.29	1.92	47	52.2
MC2020	1.59	0.186	0.721	0.452	0.34	3.19	77	85.6
DIN	1.41	0.248	0.749	0.530	0.25	3.25	59	65.6

- Table 3(b) shows the statistical properties after the first adjustment.
- Table 3(c) shows the statistical properties after the second adjustment.
- Table 4(a) shows the results from the second database consisting of 73 experimental RC ties and 104 data points.
 - Table 4(b) shows the statistical properties after the first adjustment.
- Table 5(a) shows the results from the third database consisting of 33 experimental slabs in bending and 200 data points.
 - Table 5(b) shows the statistical properties after the first and second adjustments.

4.1 | First database (beams subjected to bending)

Table 3(a) shows the modeling uncertainty for all 92 RC beams included in the reviewed literature with 429 data points. After the first adjustment, as shown in Table 3(b), and the second adjustment in Table 3(c) of the database,

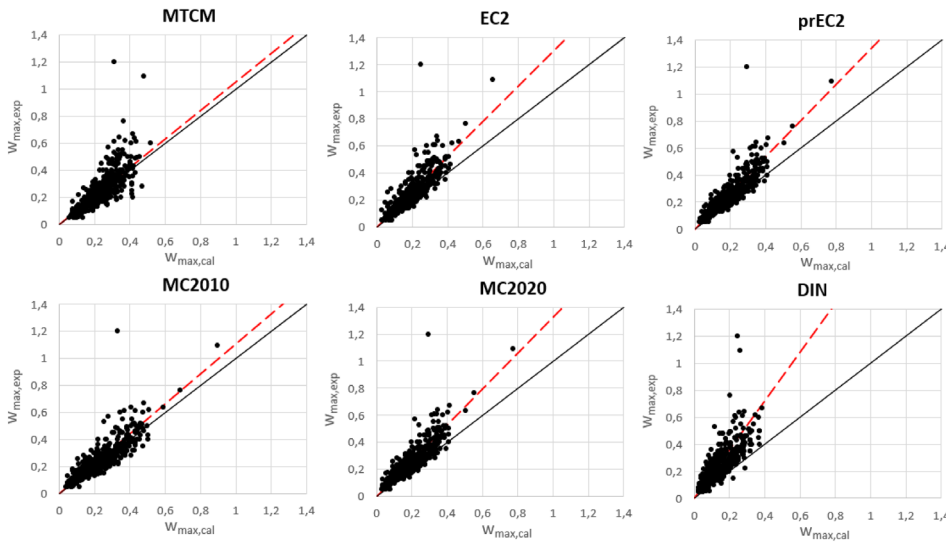


FIGURE 11 Modeling uncertainty from Table 3(a) with the long dash line (red) as the mean value (θ_{mean}), while the solid line is the 1 to 1 line.

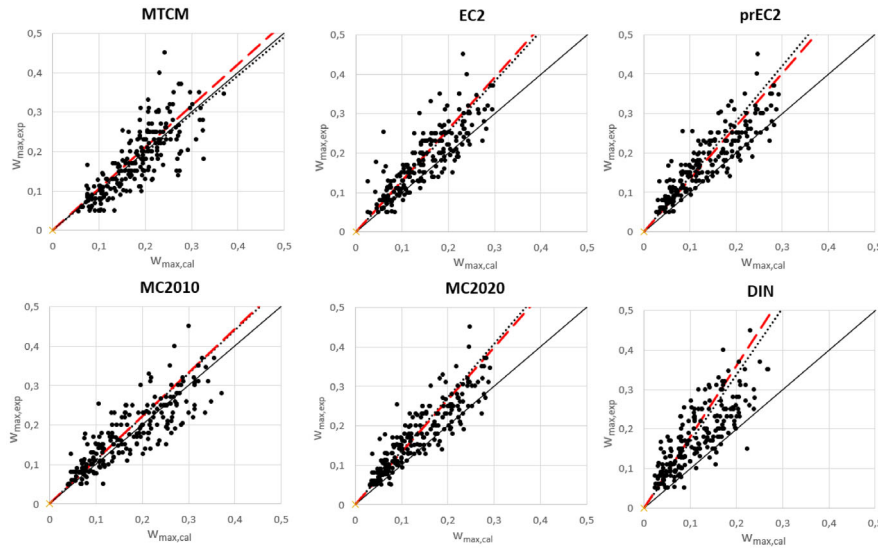


FIGURE 12 Modeling uncertainty from Table 3(c), black dotted line as the mean value, long dash line (red) as the global mean value from Table 3(a) and solid line as 1 to 1 line.

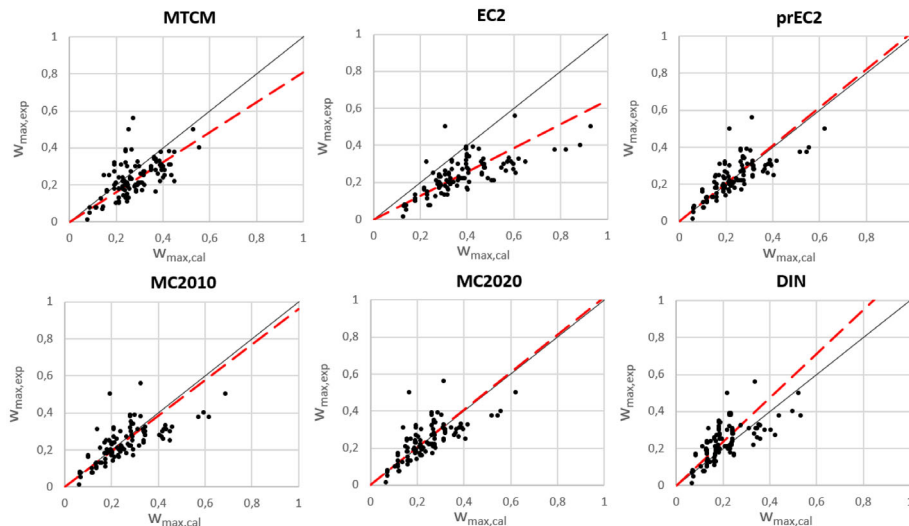


FIGURE 13 Modeling uncertainty from Table 4(a) with the red long dash line as the global mean value and solid black line as the 1 to 1 line.

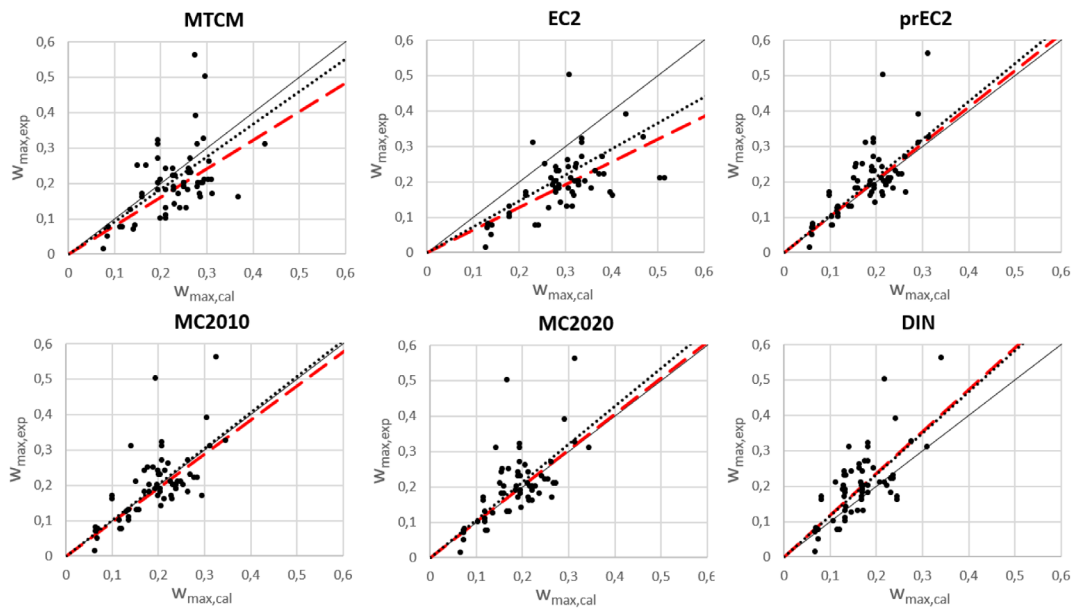


FIGURE 14 Modeling uncertainty from Table 4(b), black dotted line as the mean value, long dash line (red) as the global mean value from Table 6 and solid line as 1 to 1 line.

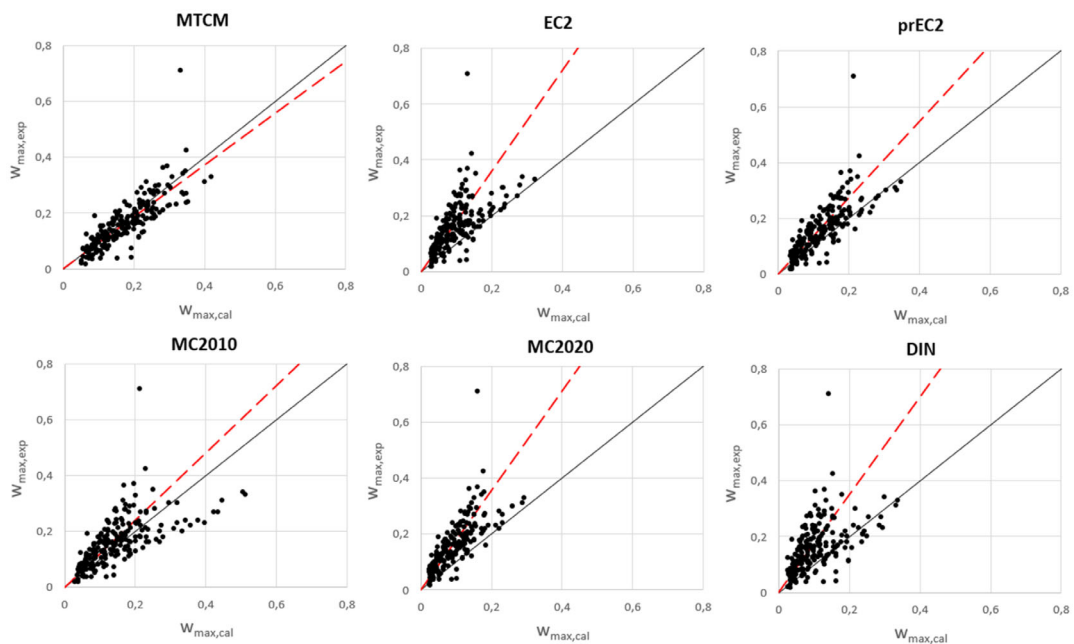


FIGURE 15 Modeling uncertainty from Table 5(a) with the long dash line (red) as the global mean value and the solid black line as 1 to 1.

we can see the change in the model uncertainties. The best agreement between the prediction models and the experiment (θ) is achieved by the MTCM and MC2010 described by θ_{mean} of 0.98 and 1.10, with an underestimated crack width in 43.3% and 57.1% of the cases. The rest of the codes has a θ_{mean} between 1.27 and 1.69 with an underestimated crack width in 79.5–95.1%

of the cases. The scatter of the prediction models and the experiment expressed by the coefficient of variation (θ_{cov}) are lowest for FprEC2 ($\theta_{cov} = 0.266$) and MC2020 ($\theta_{cov} = 0.257$) while the largest are EC2 ($\theta_{cov} = 0.29$), MTCM ($\theta_{cov} = 0.293$), and DIN ($\theta_{cov} = 0.35$). These changes are graphically illustrated in Figures 11 and 12.

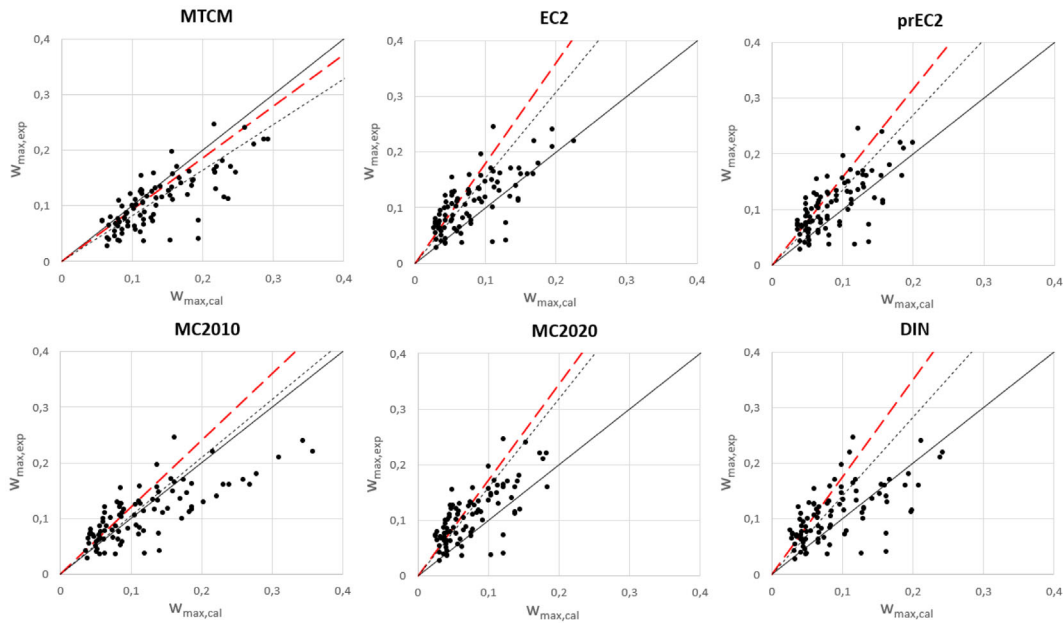


FIGURE 16 Modeling uncertainty from Table 5(b) black dotted line as the mean value, long dash line (red) as the global mean value from Table 6 and solid black line as 1 to 1.

Table 3(b) shows the modeling uncertainty after disregarding steel stresses >300 Mpa from Table 3(a).

Table 3(c) shows the modeling uncertainty after the second adjustment, disregarding the tension-stiffening effect described in Equation (28) in Table 3(b).

4.2 | Second database (RC ties in tension)

Table 4(a) shows the modeling uncertainty for all 73 RC ties included in the reviewed literature with 104 data points. After the first adjustment of the database shown in Table 4(b), we can see an improvement for almost all prediction models except for DIN, which has an increase in all statistical uncertainties except θ_{mean} . However, the reported crack spacing is the maximum at the last load level, and no other spacing was reported; therefore, the second adjustment by neglecting concrete strains, that is, tension stiffening, was not performed. The best agreement between the prediction models and the experiment (θ) expressed by θ_{mean} are MTCM, FprEC2, MC2010 and MC2020 with 0.92, 1.00, 1.07 and 1.08, respectively. The scatter of the prediction models and the experiment expressed by the coefficient of variation (θ_{cov}) are higher than for all the models in the first database with RC beams in bending with a θ_{cov} between 0.358 and 0.406.

These changes are graphically illustrated in Figures 13 and 14.

Table 4(b) shows the modeling uncertainty after the first adjustment, excluding data with stresses larger than 300 MPa.

4.3 | Third database (slabs in bending)

Table 5(a) shows the modeling uncertainty for all 33 RC slabs included in the reviewed literature with 200 data points. After the first and second adjustments of the database, we can see a change in the model uncertainties, presented in Table 5(b). The best agreement between the prediction models and the experiments (θ) are MTCM and MC2010, described by θ_{mean} of 0.82 and 1.05, while the rest of the codes has a θ_{mean} between 1.27 and 1.59. The scatter of the prediction models described by the coefficient of variation (θ_{cov}) are best for MTCM with 0.365, and the other design codes vary between 0.42 and 0.53. These changes are graphically illustrated in Figures 15 and 16.

Table 5(b) shows the modeling uncertainty after the first and second adjustments, excluding data with stresses larger than 300 MPa and disregarding the tension-stiffening effect described in Equation (28) from Table 5(a).

5 | DISCUSSION

Established databases with crack width measurements can be complicated to use for benchmarking purposes, and misinterpretations are bound to occur if special care is not taken. The complexity stems mainly from the lack of homogeneity in the measurement criteria used in different laboratories, and also because test reports are not always well documented, so it is complicated to understand the measuring procedures. In the case of crack width measurement, subjective factors may play a major role. Therefore, evaluating calculation models towards experimental results should be done with a critical view. There could be grounds for confusion between the experimental results and the analytical prediction models, as stated by Schlicke et al.¹² Therefore, the correlation between theoretical formulations and their reference to reality is necessary, and combining experimental data from various sources might be especially challenging.

5.1 | Adjustment of the database

The content and methods used to establish a comprehensive database like this could influence the results due to the nature and properties of the input data (random products), even though the statistical properties are almost homogenous for all the codes. As noted from Table 3, all models show large numbers of observations n for which the crack widths measured exceed the predicted crack width ($\theta > 1$). Such population behavior might lead to thinking that the predicted crack widths are too small or incorrect, and that the crack width values measured experimentally are too large or inconsistent. There is generally a large scatter from all models, which can be related to the aleatory uncertainties and

the subjective interpretations and choices made by the reporting authors. Observing that the statistical properties for the model uncertainties of the calculation models are in the same order of magnitude justifies these viewpoints.

Several experimental tests reported large crack widths, such as Rüsç & Rehm³²: For Beam No R-69, a maximum crack width of 1.2 mm at 390 MPa was reported, while the average crack width from the prediction models was 0.27 mm. The reported reinforcement yield stress was 400 MPa. Therefore, plastic deformation in the steel could have affected the crack and supported the choice for the first adjustment. Even if the difference in terms of maximum crack width given by the prediction model was irrelevant, it is evident how such outliers can affect the modeling uncertainty; hence, the need to benchmark the models.

Table 6 shows that 28 data points from 14 beams tested by Rüsç & Rehm³² exceed the theoretical maximum mean crack width given in Equation (35), and 90 data points by Clark,³³ as shown in Table 7.

As seen in Table 8 and Figures 17 and 18, it is complicated to interpret crack spacings from the experimental tests consistently. To improve the accuracy of the second adjustment for Rüsç & Rehm, the experimental results would require detailed interpretations of the crack patterns. A solution strategy could be to determine maximum- and average crack widths and spacings based on their size and crack propagation into the effective tensile zone, that is, if a crack width is constant and not increasing its propagation in the beam height with increased reinforcement stress, the crack would be disregarded as a secondary crack. Different interpretations of crack spacings may not be wrong, but to achieve consistent results, the same basis of interpretation should be used for all experimental tests.

TABLE 6 Number of experimental data points exceeding the mean crack width criterion (neglecting tension stiffening).

Criteria	Hognestad	CUR-report	Rusch-Rehm	Clark	Total numbers
$w_{k,mean} < \varepsilon_{sr} S_{r,mean,exp}$	114	92	41	64	311
$w_{k,mean} > \varepsilon_{sr} S_{r,mean,exp}$	0	0	28	90	118

Note: $S_{r,mean,exp}$ is based on different interpretations of crack spacings for each database.

TABLE 7 Number of experimental beams where the mean crack width requirement is exceeded for at least one data point.

Criteria	Hognestad	CUR-report	Rusch-Rehm	Clark	Total numbers
$w_{k,exp} < \varepsilon_{sr} S_{r,mean,exp}$	30	24	4	1	59
$w_{k,exp} > \varepsilon_{sr} S_{r,mean,exp}$	0	0	10	23	33

Note: $S_{r,mean,exp}$ is based on different interpretations of crack spacings for each database.

TABLE 8 Experimental Beam R-69 by Rüsç & Rehm.

Beam	MTCM	EC2	prEC2	MC2010	MC2020	DIN	Experimental results				Conservative mean
							Reported	σ_{sr}	$w_{k,max}$	$w_{k,mean}$	
R-69	w_k (mm)						$S_{r,mean}$ mm	σ_{sr} MPa	$w_{k,max}$ mm	$w_{k,mean}$ mm	$w_{k,mean} = \epsilon_{sr} S_{r,mean}$
	0.14	0.12	0.14	0.14	0.14	0.12	150	200	0.15	0.07	0.15
	0.18	0.15	0.18	0.18	0.18	0.15	115	250	0.23	0.11	0.14
	0.22	0.19	0.22	0.23	0.22	0.19	105	300	0.25	0.13	0.16
	0.26	0.22	0.26	0.27	0.26	0.22	102	350	0.3	0.16	0.18
	0.29	0.25	0.30	0.30	0.30	0.25	100	390	1.2	0.23	0.20

Note: $w_{k,max}$ is the maximum crack width at the bottom face by the average value of five measured points I, II, III, IV, and V.

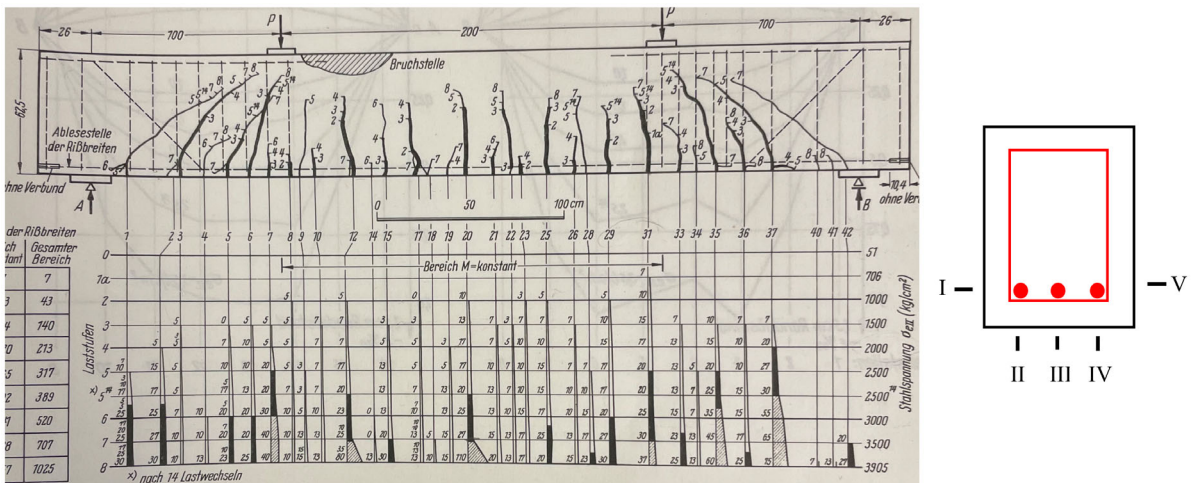


FIGURE 17 Crack widths for R-69 (in 1/100 mm) with corresponding load intensity on one side of the beam with the crack width reading at point V.

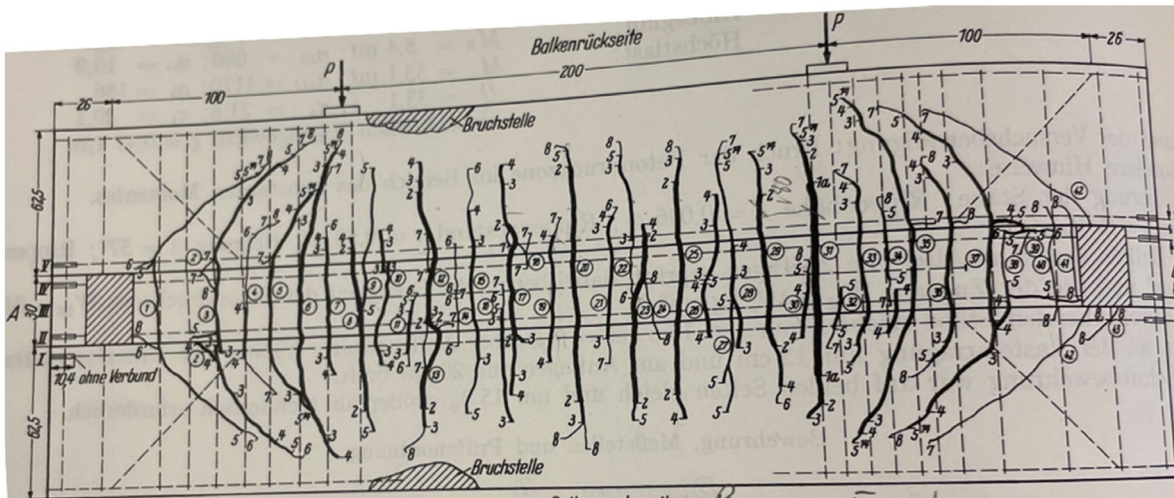
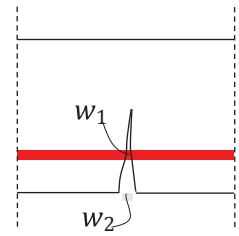


FIGURE 18 Illustration of cracks on the beam faces of R-69, crack number and load intensity 1-8.

TABLE 9 Predicted crack width location.

Model	Description	
EC2	w_2	At the outermost concrete face
FprEC2	w_2	At the outermost concrete face
MC2010	w_1, w_2	At reinforcement height and outermost concrete face.
MC2020	w_2	At reinforcement height and outermost concrete face.
MTCM	—	Representative crack width over the surface of the effective tensile area
DIN	—	Representative crack width over the surface of the effective tensile area



5.2 | Crack width location

The crack width predicted by the investigated models does not represent the crack width at the same location, as seen in Table 9. MC2010 determines the crack width at the reinforcement height with the option to extrapolate to the outermost concrete surface. The current EC2 does not directly state the predicted crack width location; however, the work described in fib bulletin 92⁴⁰ supports that the predicted crack width is at the outermost concrete face. In FprEC2, it is now directly stated that the crack width is at the outermost concrete face. The German annexe to EC2 (DIN) is based on Model Code 1990,⁴¹ which takes no explicit account of cover and is based primarily on defining the transfer length based on rebar size and reinforcement ratio, which includes no explicit empirical cover term like the formulations in the TCM and MTCM. The predicted crack width by DIN and MTCM is a representative maximum crack width over the effective tensile area.

5.3 | Effective concrete area

For beams in bending, EC2 and MC2010 define the effective height as.

$$h_{ef} = \min\left(2.5(h-d); \frac{h-x}{3}\right) \quad (37)$$

In both cases, the effective height limitation $(h-x)/3$ is included to distinguish between elements in bending and tension. The explanation for this limitation is based on the stress distribution over the cross-section height in bending; however, as pointed out by Reference 42, there seems to be no published justification for this factor which seems to be originating from curve fitting to test data. Therefore, when calculating the effective height by

MTCM, the effective height was defined as $h_{ef} = 2.5(h-d)$ for beams and slabs in bending.

For RC ties in tension, MTCM applies the EC2 and MC2010 definitions:

$$h_{ef} = \min\left(2.5(h-d); 2.5\left(c + \frac{\phi_s}{2}\right); \frac{h}{2}\right) \quad (38)$$

5.4 | The difference in bond stress and crack spacing formulas by the models

The applied codes EC2, Model Codes and DIN assume that the bond stresses are proportional to the concrete's tensile strength with the assumption of a perfectly plastic bond-slip relation, as shown in Figure 1. MC2010 and DIN apply constant mean bond stresses equal to 1.8 times the tensile strength of concrete ($\tau_{sm} = 1.8f_{ctm}$), while EC2 applies 2.5 or 1.25 depending on if deformed or smooth bars are used. This assumption means that the bond stress is independent of the slip between rebar and concrete, and the effects of geometry and stress level are not directly considered. In contrast, MTCM yields different mean bond stresses directly dependent on the slip where geometry and stress level are accounted for. This effect is illustrated in Figure 19 for constant reinforcement ratio versus increasing rebar stress and different rebar sizes.

Another major difference between MTCM and the code formulations that should be highlighted is how the transfer length in the crack formation stage is accounted for. No explicit term is provided for the code formulations, while MTCM provides a solution method by means of the CLLM behavior. Capturing this behavior has previously proven essential for sections with large covers, as stabilized cracking might not be obtained even for relatively large steel stresses.³⁰ The transfer lengths

between formed cracks will not overlap and interfere in such cases. This will, for instance, lead to incorrect and inconsistent calibration of code formulations if such spacing between cracks is interpreted as a specific maximum crack spacing. Unlike the code formulations, MTCM does not use the crack spacing as a primary variable determined a priori to calculate the crack width but rather deduced from the calculations as a state variable. This means that only the maximum crack width is the primary variable returned from an MTCM calculation. The authors are thus of the opinion that the calculated transfer lengths of each side of a crack are more critical than the crack spacing measured itself. Two further develop this opinion, two parametric studies were carried out for Hognestad B-5, the first shown in Table 10, with increased concrete cover as the only variable. The results for predicted crack spacing are shown in Figure 20 for MTCM and EC2.

The second study was performed for the same beam with increased cover sizes and keeping the reinforcement ratio constant by increasing the reinforcement diameter,

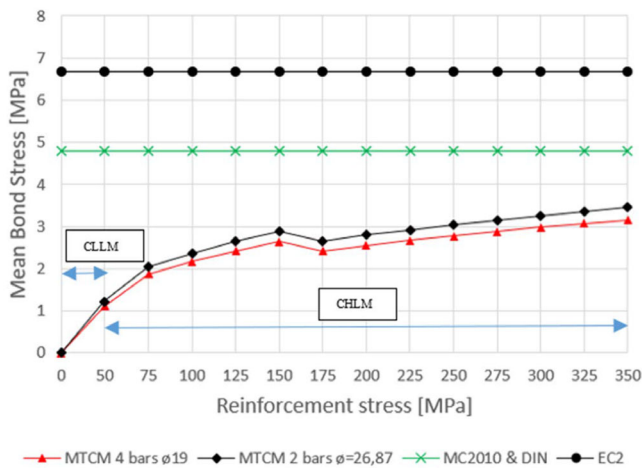


FIGURE 19 Bond stresses for different rebar sizes with constant reinforcement ratio between MTCM, EC2, MC2010 and DIN for Hognestad Beam No 5.

TABLE 10 Parametric study of increased cover with effective depth kept constant for Hognestad B-5 beam.

Hognestad B-5, 4ø19					
Width (mm)	Height (mm)	Effective depth (mm)	$h_{ef} = 2.5(h - d)$ (mm)	Cover (mm)	ρ_{ef} (%)
203	406 ^a	360	115	25	4.86
	430		174	50	3.22
	455		236	75	2.46
	480		299	100	2.33
	505		361	125	2.21

^aTested beam.

as shown in Table 11. The results for predicted crack spacing are shown in Figure 21 for MTCM and EC2.

Figures 20 and 21 show that the crack formation stage (CLLM) and the stabilized cracking stage (CHLM) in MTCM heavily depend on the reinforcement ratio and rebar size. The difference between predicted crack spacing in the stabilized cracking stage of MTCM and Eurocode 2 is even more significant for large-scale concrete structures, which could yield maximum crack spacing up to over 1 m with large covers, small rebars and a low reinforcement ratio. This would, in practice, never be the case as crack spacing for stabilized cracking rarely becomes larger than half a meter, justifying the code formulation's inconsistency.

The aforementioned oversimplifications made by the codes result in the effect of cracking only being captured by empirical calibration of the predicted crack spacing. Considering that the empirical calibration is performed with respect to a specific database suggests that the code formulation cannot capture the cracking behavior of an arbitrary section properly judged from a mechanical viewpoint. This further implies that the formulation in the codes should have a strictly limited range of applications and that care should be taken when applying the calculations, in particular to cross-sections with properties deviating from those in the database, for example, cross-sections with large heights, covers, rebars or the combination of them. Figures 22 and 23 compare measured crack width versus calculated crack widths for databases 1 and 2 when the data are separated into normal and large covers.

In the case of MTCM, for beams in bending with cover in the range of 38–48 mm, shown in Figure 22, the predicted crack width is in good agreement with experimental data. However, with larger concrete covers in the 51–102 mm range, the predicted crack width is underestimated. Both DIN and MTCM transform an arbitrary cross-section into an equivalent cross-section. Furthermore, DIN solves this problem by assuming a constant bond stress distribution while MTCM acknowledges that

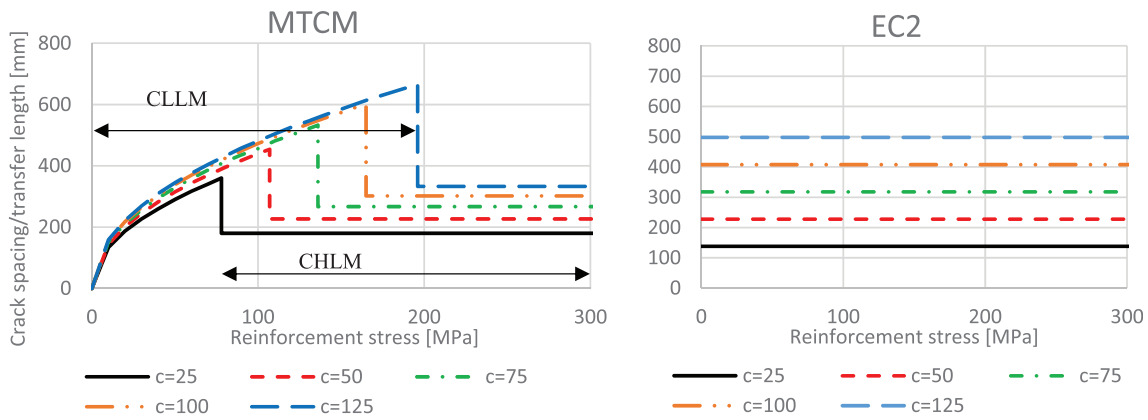


FIGURE 20 Crack spacing/transfer length for MTCM and EC2 for different cover sizes of Hognestad B-5 beam with values from Table 10.

TABLE 11 Parametric study of increased cover with effective depth and reinforcement ratio kept constant with different rebar sizes for Hognestad B-5 beam.

Hognestad B-5, constant reinforcement ratio, $n = 4$						
Width (mm)	Height (mm)	Effective depth (mm)	$h_{ef} = 2.5(h - d)$ (mm)	Cover (mm)	σ_s (mm)	ρ_{ef} (%)
203	406 ^a	360	115	25	19.00	4.86
	432		180	50	23.76	
	459		247	75	27.86	
	486		314	100	31.43	
	512		381	125	34.58	

^aTested beam.

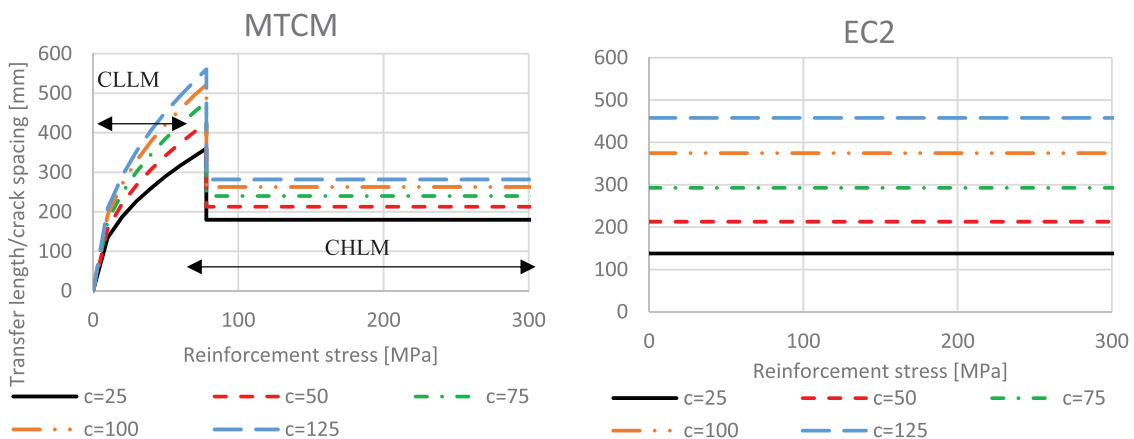


FIGURE 21 Crack spacing/transfer length for MTCM and EC2 for different cover sizes of Hognestad B-5 beam with values from Table 11.

the bond stress distribution around the rebar is not uniform in a non-symmetric RC tie by applying the parameter $\psi = 0.7$. However, a considerable difference between the vertical and horizontal concrete cover, which was 25 mm for the case of 63 and 102 mm vertical cover, is a

natural explanation for the considerable underestimation of the crack width in these cases for both DIN and MTCM. It is also seen that MTCM performs well in cases of a relatively small difference in vertical and horizontal covers. For the RC ties in tension shown in Figure 23,

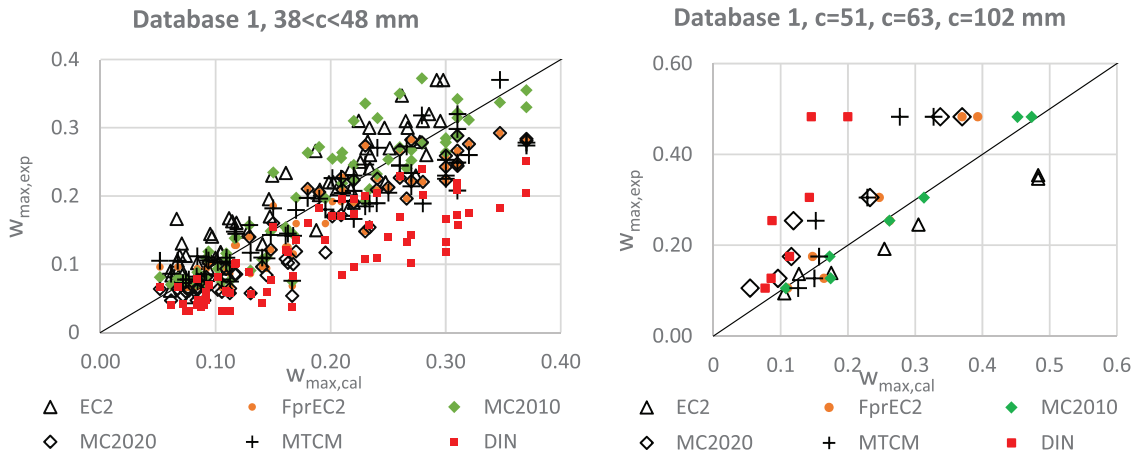


FIGURE 22 Comparison of measured crack width with calculated crack width for Database 1 with different concrete covers.

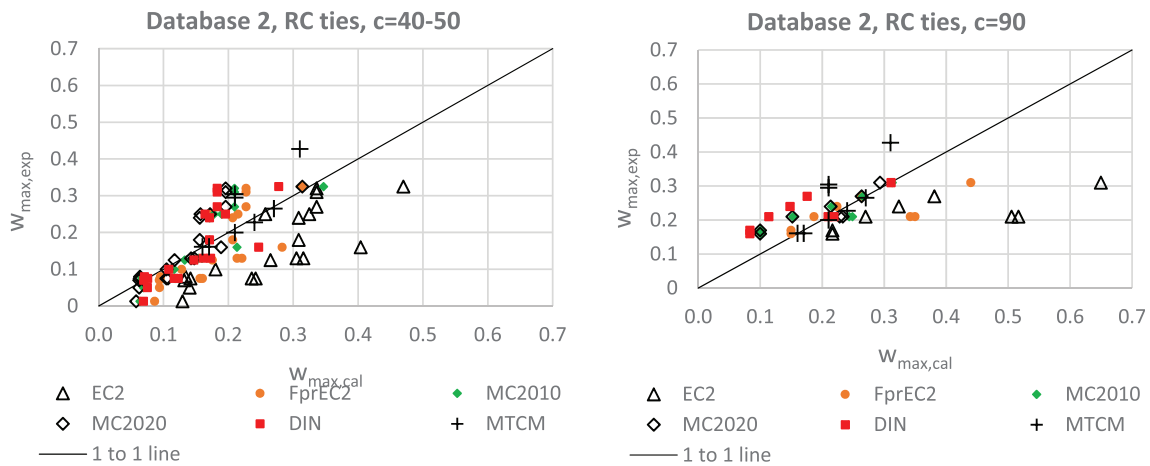


FIGURE 23 Comparison of measured crack width with calculated crack width for Database 2 with different concrete covers.

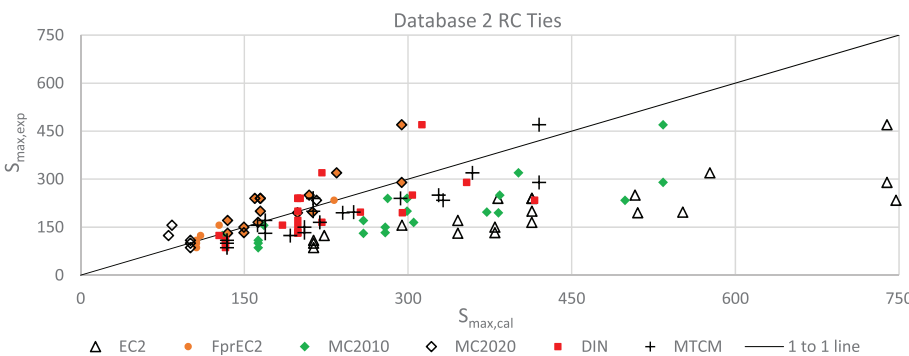


FIGURE 24 Measured maximum crack spacing versus calculated maximum crack spacing for reported values in Database 2 cover sizes of 20–90 mm.

there is perfect symmetry in all cases regarding vertical and horizontal cover, and both DIN and MTCM are in good agreement with the experimental results for both normal and large concrete covers.

Figure 24 shows the maximum measured crack spacing versus calculated crack spacing with clear indications

that EC2 and MC2010 overestimate the crack spacing for RC ties. The MTCM predict the crack width and spacing for RC ties to a good extent, even though the crack spacing is not a primary variable in the MTCM.

The MTCM is purely based on a mechanical formulation and has not been calibrated towards any

experimental databases at all. Observing that it performs as well as the code formulations, not to say even better, suggests that it (i) offers a wider range of applications and, thus, (ii) shows greater potential for development than the codes. The current drawback is that the MTCM calls for a numerical solution procedure, which makes it more complicated to handle for a code type formulation and daily use for design purposes. This also makes sense since it is a refined calculation model compared to the code formulations. Hence, this calls for the development of a simplified version of the MTCM, which can be compressed to a code-type formulation for the purpose of becoming a direct competitor to the current code formulations. This can be obtained by applying the mechanical basis in the MTCM to formulate a closed-form solution for the CHLM case instead of a non-closed solution. The authors of this article are currently working on developing such a model.

6 | CONCLUSIONS

This article shows the performance of the crack width calculation methods according to Eurocodes (EC2, FPrEC2), *fib* Model Codes, German Annex to Eurocode 2 and the new MTCM, applying the principles of model uncertainty. The calculation methods are benchmarked against experiments performed by various authors in the literature, which further was collected into a comprehensive database consisting of 429 data points obtained from bending tests of beams, 104 data points obtained from tensile tests of RC ties and 200 data points obtained from bending tests of slabs. The modeling uncertainty shows that the MTCM performs best for beams in bending with $\theta_{\text{mean}} = 0.98$, for MC2010 RC ties in tension with $\theta_{\text{mean}} = 1.0$ and for slabs in bending with $\theta_{\text{mean}} = 1.05$. DIN underestimate the crack width to a relatively large extent for beams in bending with $\theta_{\text{mean}} = 1.69$. The majority of the experimental tests in the database have already been used to develop the code formulations by means of empirical calibration.

The crack width models compared are based on the same theoretical framework expressing the crack width as a product of crack spacing and strain difference between reinforcement and concrete. However, the models incorporate mechanical properties such as bond stress distribution, effective tension area, strain gradients and consideration of the crack stages differently. In addition, Eurocode 2 and Model Code use empirical modifications to adjust the calculated crack width, that is, cover term in the crack spacing formulas. The reason behind this is justified from an empirical standpoint in the literature,^{43–47} which clearly shows that cover is a

significant factor in crack spacing. The proposed changes from EC2 to FpEC2 are well documented by Caldentey et al.⁴² The first and third databases have a majority of the experimental members with relatively small covers of 20–30 mm and 10–20 mm which do not favor the new empirical k_{fl} factor in MC2020 and FPrEC2 intended to account for the effect of stress distribution within the effective concrete tensile area. Therefore, the authors of this article find it challenging to conclude the general effect of the new empirical and mechanical modifications from the results included in the existing databases. It can however be argued, from a mechanical viewpoint, that the largest inconsistencies in the code formulations stem from the oversimplifications of (i) an excessive focus on crack spacing rather than the maximum crack width itself and (ii) assuming constant bond stress regardless of geometry and stress level. The lack of mechanical understanding and interpretation in the code formulation is compensated for by experimental calibration against a chosen database. This will provide a strict range of applicability. In contrast, the results in this article show that the MTCM performs as well as the code formulations without calibration towards a specific database.

7 | SUGGESTIONS FOR FURTHER RESEARCH

The findings in this article suggest that a simplified version of the MTCM should be developed to obtain a code-type formulation that can challenge the current code formulations investigated in this study. The first step in this approach would be to obtain a closed-form solution in the case of CHLM in the MTCM. The authors are currently working on such a calculation model.

DATA AVAILABILITY STATEMENT

The data that support the findings of this study are available from the corresponding author upon reasonable request.

ORCID

Reignard Tan  <https://orcid.org/0000-0001-8190-6215>

REFERENCES

- Leonhardt F. Zur Behandlung von Rissen im Beton in den deutschen Vorschriften (Teil 1). Ther Ber. 1985;80:179–84.
- Beeby AW. Corrosion of reinforcing steel in concrete and its relation to cracking, vol. 56A. London: Institution of Structural Engineers; 1978. p. 77–81. <https://trid.trb.org/view/78946>
- Basteskår M, Engen M, Kanstad T, Fosså KT. A review of literature and code requirements for the crack width limitations for design of concrete structures in serviceability limit states. Struct

- Concr. 2019;20(2):678–88. Portico. <https://doi.org/10.1002/suco.201800183>
4. Borosnyói A, Balázs GL. Models for flexural cracking in concrete: the state of the art. *Struct Concr.* 2005;6(2):53–62. <https://doi.org/10.1680/stco.2005.6.2.53>
 5. Basteskår M, Engen M, Kanstad T, Johansen H, Fosså KT. Serviceability limit state design of large concrete structures: impact on reinforcement amounts and consequences of design code ambiguity. *Eng Struct.* 2019;201:109816. <https://doi.org/10.1016/j.engstruct.2019.109816>
 6. CEN. EN 1992-1-1, Eurocode 2: Design of Concrete Structures—Part 1-1: general rules and rules for buildings. Brussels: European Committee for Standardization; 2004.
 7. CEN-TC250-SC2-WG1_N1296_FprEN_1992-1-1_e_stf_2022-07-24 FIN clean. 2022.
 8. fib. Model Code for Concrete Structures 2010. Berlin: International Federation for structural concrete; 2013.
 9. 2nd Draft of ModelCode 2020—December. 2022.
 10. DIN: EN-1992-1-1/NA. 2011-01, National Annex—Nationally determined parameters—Eurocode 2: Design of concrete structures—Part 1-1: General rules and rules for buildings. 2011.
 11. Tan R, Hendriks MAN, Geiker M, Kanstad T. Analytical calculation model for predicting cracking behavior of reinforced concrete ties. *J Struct Eng.* 2020;146(2):04019206. <https://doi.org/10.1061/%28ASCE%29ST.1943-541X.0002510>
 12. Schlicke D, Dorfmann EM, Fehling E, Tue NV. Calculation of maximum crack width for practical design of reinforced concrete. *Civ Eng Des.* 2021;3(3):45–61. <https://doi.org/10.1002/cend.202100004>
 13. Tan R. Consistent crack width calculation methods for reinforced concrete elements subjected to 1D and 2D stress states a mixed experimental, numerical and analytical approach, Philosophiae Doctor, Department of Structural Engineering, Norwegian University of Science and Technology. 2019 <http://hdl.handle.net/11250/2607051>
 14. Terjesen O, Kanstad T, Tan R. Application of NLFEA for crack width calculations in SLS. In: Meschke G, Pichler B, Rots JG, editors. *Computational modelling of concrete and concrete structures*. 1st ed. Vienna: Routledge Taylor & Francis Group; 2022. p. 246–54. <https://www.routledge.com/Computational-Modelling-of-Concrete-and-Concrete-Structures/Meschke-Pichler-Rots/p/book/9781032327242#>
 15. Cervenka V, Rimkus A, Gribniak V, Cervenka J. Simulation of the crack width in reinforced concrete beams based on concrete fracture. *Theor Appl Fract Mech.* 2022;121:103428. <https://doi.org/10.1016/j.tafmec.2022.103428>
 16. Naotunna CN, Samarakoon SMSMK, Fosså KT. Experimental investigation of crack width variation along the concrete cover depth in reinforced concrete specimens with ribbed bars and smooth bars. *Case Stud Construct Mater.* 2021;15:e00593. <https://doi.org/10.1016/j.cscm.2021.e00593>
 17. Beeby AW, Scott RH. Cracking and deformation of axially reinforced members subjected to pure tension. *Magaz Concr Res.* 2005;57(10):611–21. <https://doi.org/10.1680/macrc.2005.57.10.611>
 18. Beeby RHSAW. Influence of tension stiffening on deflection of reinforced concrete structures: report of a concrete society. Sandhurst, Berkshire: Concr Soc; 2004.
 19. Beeby AW. The influence of the parameter ϕ/ϕ_{eff} on crack widths. *Struct Concr.* 2005;6:155–65. <https://doi.org/10.1680/stco.2005.6.4.155>
 20. Russo G, Romano F. Cracking response of RC members subjected to uniaxial tension. *J Struct Eng.* 1992;118(5):1172–90. [https://doi.org/10.1061/\(ASCE\)0733-9445\(1992\)118:5\(1172\)](https://doi.org/10.1061/(ASCE)0733-9445(1992)118:5(1172))
 21. fib. Bond of reinforcement in concrete: state-of-art report fib bulletin No. 10. Lausanne, Switzerland: Sprint-Druck Stuttgart; 2000.
 22. Marti P, Alvarez M, Kaufmann W, Sigrist V. Tension chord model for structural concrete. *Struct Eng Int.* 1998;8(4):287–98. <https://doi.org/10.2749/101686698780488875>
 23. Alvarez M. Einfluss des Verbundverhaltens auf das Verformungsvermögen von Stahlbeton. Birkhäuser. 1998;236:3-7643-5993-5.
 24. Edwards AD, Picard A. Theory of cracking in concrete members. *Proc ASCE J Struct Div.* 1972;98(12):2687–700.
 25. Tan R, Hendriks MAN, Kanstad T. An investigation of the strain profile over the cover in reinforced concrete elements subjected to tension. 5th fib Congress in Melbourne, Australia (2018) proceedings, 7-11 October, Melbourne Australia; 2019. p. 1784–91.
 26. Eligehausen R, Popov EP, Bertero VV. Local bond stress-slip relationships of deformed bars under generalised excitations: experimental results and analytical model. Rep. No. UCB/EERC 83/23. Berkeley, CA: University of California. 1983.
 27. Tan R, Hendriks MAN, Geiker M, Kanstad T. A numerical investigation of the cracking behaviour of reinforced-concrete tie elements. *Mag Concr Res.* 2020;72(3):109–21. <https://doi.org/10.1680/jmacr.18.00156>
 28. Caldentey AP, García R, Gribniak V, Rimkus A. Tension versus flexure: reasons to modify the formulation of MC 2010 for cracking. *Struct. Concr.* 2020;21(5):2101–23. <https://doi.org/10.1002/suco.202000279>
 29. Stable version CEN-TC250-SC2-WG 102_N0321_CENTC_250SC_2_WG_1_N_1143_- Stable_version_of_prEN_1992-1-1:2021-09. 2022.
 30. Hognestad. Journal of PCI Research and Development Laboratories. 1962. 1962.
 31. CUR. Dutch centre for civil engineering, Research and Codes Report no. 37 (Out of print). 1994.
 32. Rüsç EH, Rhem G. Versuche mit BetonformStählen. (1963), pt. II (1963), pt. III (1964). Deutscher Ausschuss für Stahlbeton, No. 140. 1963–1964.
 33. Clark AP. Cracking in reinforced concrete flexural members. *ACI J, Proc.* 1956;27(8):851–62.
 34. Hartl G. Die Arbeitslinie " eingebetteter Stähle" bei Erst- und Kurzzeitbelastung Dissertation, University of Innsbruck. 1977.
 35. Rimkus A. Effects of Bar reinforcement arrangement on deformations and cracking of concrete elements. Doctoral Dissertation. Vilnius: Technika, 2017. 143 p. 2017.
 36. Wu H, Gilbert R. An experimental study of tension stiffening in reinforced concrete members under short-term and long-term loads. 2008.
 37. Tan R, Eileraas K, Opkvitne O, Žirgulis G, Hendriks MAN, Geiker M, et al. Experimental and theoretical investigation of crack width calculation methods for RC ties. *Struct Concr.* 2018;19(5):1436–47. <https://doi.org/10.1002/suco.201700237>.
 38. Engen M, Hendriks MAN, Köhler J, Øverli JA, Åldstedt E. A quantification of the modelling uncertainty of nonlinear finite element analyses of large concrete structures. *Struct Saf.* 2017; 64:1–8. <https://doi.org/10.1016/j.strusafe.2016.08.003>

39. JCSS. Probabilistic model code, 12th draft. joint committee on Structural Safety. 2001.
40. Serviceability limit state of concrete structures: Technical report fib bulletin 92. 2019.
41. Euro-International Committee for Concrete. Ceb-Fip model code 1990: design code. Thomas Telford. 1991.
42. Caldentey A, Bellod J, Torres L, Kanstad T. Serviceability limit states according to the new Eurocode 2 proposal: description and justifications of the proposed changes. *Hormigón y Acero*. 2023;71:91–108. <https://doi.org/10.33586/hya.2023.3104>
43. Guedes F, and Vaz Rodrigues R, The effect of concrete cover on the crack width in reinforced concrete members—a code perspective. 2nd International Conference on Recent Advances in Nonlinear Models-Design and Rehabilitation of Structures, Coimbra, Portugal 2017. https://www.uc.pt/ctuc/dec/destaques_historico/CoRASS
44. Naotunna C, Samarakoon S, Fosså K. A new crack spacing model for reinforced concrete specimens with multiple bars subjected to axial tension using 3D nonlinear FEM simulations. *Struct Concr*. 2021;22:3241–54. <https://doi.org/10.1002/suco.202100025>
45. Naotunna C, Samarakoon S, Fosså K. Influence of concrete cover thickness and clear distance between tensile bars on crack spacing behavior of large-scale reinforced concrete members. *Fatigue Fract Eng Mater Struct*. 2022;45:1052–64. <https://doi.org/10.1111/ffe.13650>
46. Gribniak V, Rimkus A, Pérez Caldentey A, Sokolov A. Cracking of concrete prisms reinforced with multiple bars in tension: the cover effect. *Eng Struct*. 2020;220:110979. <https://doi.org/10.1016/j.engstruct.2020.110979>
47. Pérez Caldentey A, Corres Peiretti H, Peset Iribarren J, Giraldo Soto A. Cracking of RC members revisited: influence of cover, ϕ/ρ_s , e_f and stirrup spacing: an experimental and theoretical study. *Struct Concr*. 2013;14(1):69–78. <https://doi.org/10.1002/suco.201200016>

AUTHOR BIOGRAPHIES



Otto Terjesen, M.Sc. PhD Research Fellow, University of Agder, Jon Lilletuns vei 9, 4879 Grimstad, Norway.
Email: otto.terjesen@uia.no



Gianclaudio Pinto, M.Sc. Civil Engineer, Implenia Norway AS, Fornebuveien 11, 1366, Oslo, Norway.
Email: gianclaudio.pinto@implenia.com



Terje Kanstad, Ph.D., M.Sc, Professor, Norwegian University of Science and Technology, Richard Birkelands vei 1A, 7491 Trondheim, Norway.
Email: terje.kanstand@ntnu.no



Reignard Tan, Ph.D., M.Sc. Associate Professor, Norwegian University of Science and Technology, Richard Birkelands vei 1A, 7491 Trondheim. Multiconsult AS, Postboks 265 Skøyen, 0213 Oslo, Norway.
Email: reignard.tan@multiconsult.no

How to cite this article: Terjesen O, Pinto G, Kanstad T, Tan R. Performance study of crack width calculation methods according to Eurocodes, *fib* model codes and the modified tension chord model. *Structural Concrete*. 2024. <https://doi.org/10.1002/suco.202300367>